The manipulation of DC, specialized antigen-presenting cells, is a promising strategy to improve the efficacy of cancer immunotherapy.[11,12] Genetic modification to express antigenic proteins has several advantages in comparison with using a peptide, protein, or tumor cell lysate as a means for loading TAA to DC.[13] The expression of TAA by DC circumvents the need for identifying specific CTL epitopes within the protein, and the antigens are continuously supplied for presentation as opposed to a single pulse of peptides or tumor cell lysates.[14] Furthermore, in vivo transfer of DC transfected with TAA gene are able to prime CTL reactive to multiple TAA-derived epitopes.[15] Others and we have established to generate DC in vitro from mouse embryonic stem (ES) cells (ES-DC).[16,17] ES-DC have the capacity to stimulate T cells, present antigen, and migrate to lymphoid tissues upon in vivo administration, and their capacity is comparable with that of bone marrow-derived DC.[15,17–19] The genetic modification of ES-DC can be carried out without the use of viral vectors by introducing exogenous genes into undifferentiated ES cells by electroporation and the subsequent induction of their differentiation into ES-DC. In a previous study, ES-DC expressing GPC3 showed protective immunity against mouse melanoma, however, the therapeutic effects were insufficient.[15] To counter the cancers with deficiencies in antigen presentation machineries, it is necessary to induce the innate immunity. Alpha-galactosylceramide (α-GalCer) presented by DC efficiently stimulates natural killer T (NKT) cells.[20] Therefore, it is presumed that the in vivo transfer of DC simultaneously loaded with TAA and α-GalCer may stimulate both tumor-reactive T cells and NKT cells, resulting in a potent anticancer immunity. The present study investigated the anticancer effects of multiple TAA-targeted immunotherapies with α-GalCer–loaded and genetically engineered ES-DC against mouse melanoma.

## MATERIALS AND METHODS

### Mice

C57BL/6 mice were obtained from Japan SLC Inc. (Hamamatsu, Japan) and maintained under specific pathogen-free conditions. All studies were performed with C57BL/6 mice syngeneic to the mouse ES cell line B6 at 6 to 8 weeks of age. The mouse experiments were approved by the Animal Research Committee of Kumamoto University.

### Cell Lines

The ES cell line B6, derived from C57BL/6 blastocysts, was kindly provided by Drs H. Suemori and N. Nakatsuji (Kyoto University). The method for in vitro induction of differentiation of ES cells into DC was described previously,[17] and ES-DC prepared from a 7-day culture in the presence of granulocyte-macrophage colony-stimulating factor were used for all assays. The C57BL/6-derived tumor cell lines, F10 and BL6 sublines of B16 melanoma, a fibrosarcoma cell line MCA205 (MCA), and a thymoma cell line EL-4 were provided by the Cell Resource Center for Biomedical Research Institute of Development, Aging, and Cancer, Tohoku University (Sendai, Japan). The cells were cultured in Roswell Park Memorial Institute-1640 supplemented with 10% horse serum. To produce GPC3-expressing MCA (MCA-GPC3), MCA cells were transfected with pCAGGS-GPC3-internal ribosomal entry site (IRES)–puromycin-resistant (puro-R) by using Lipofectamine 2000 (Invitrogen, Carlsbad, CA), selected with puromycin, and then subjected to cloning by limiting dilution as described previously.[15,21] To produce EL-4–expressing secreted protein acidic and rich in cysteine (EL-4–SPARC), EL-4 cells were transfected with pCAGGS-SPARC-IRES–puro-R same as above. Plasmid DNA encoding firefly luciferase was kindly provided by Dr M. Nishikawa (Kyoto University), and B16-BL6 cells were transfected with the construct as described above, then the single colonies of G418-resistant cells were picked up, and a clone was selected on the basis of the luciferase activity (B16-BL6/Luc).

### Peptides and Cytokines

Known $CD8^+$ T-cell epitope peptides were purchased from AnyGen (Gwangju, Korea) and their amino acid sequences are as follows: mouse $TRP2_{180\text{-}188}$ (SVYDFFVWL, $H\text{-}2K^b$ restricted), mouse $gp100_{25\text{-}33}$ (EGSRNQDWL, $H\text{-}2D^b$ restricted), and human $gp100_{25\text{-}33}$ (KVPRNQDWL, $H\text{-}2D^b$ restricted). A control peptide derived from $OVA_{257\text{-}264}$ (SIINFEKL, $H\text{-}2K^b$ restricted) was synthesized by the automatic peptide synthesizer (PSSM8, SHIMADZU, Kyoto, Japan) and subsequently purified by high-performance liquid chromatography. Recombinant mouse granulocyte-macrophage colony-stimulating factor, recombinant human interleukin (IL)-2, recombinant murine interferon (IFN)-γ (PeproTechLondon, UK), and IL-4 (ProSpecTechnoGene, Rehovot, Israel) were purchased. Alpha-GalCer was kindly provided by Kirin Brewery Co (Tokyo, Japan).

### Generation of ES-DC expressing GPC3, SPARC, TRP2, or Human gp100

cDNA fragments encoding for total mouse SPARC and TRP2 were obtained by reverse transcription polymerase chain reaction (RT-PCR) from B16-F10. Full-length mouse GPC3 and human gp100 (hgp100) cDNA clones were purchased from Invitrogen. cDNA fragments encoding the whole GPC3 protein and a fragment of hgp100 ($hgp100_{1\text{-}300}$) including the $H\text{-}2D^b$–restricted epitope ($hgp100_{25\text{-}33}$) were isolated from those clones. cDNA for GPC3, SPARC, TRP2, or hgp100 was transferred to a mammalian expression vector pCAGGS-IRES–puro-R, containing the CAG promoter and an IRES–puro-R gene cassette,[22,23] to generate an expression vector for GPC3, SPARC, TRP2 and hgp100, pCAGGS-GPC3-IRES–puro-R, pCAGGS-SPARC-FLAG-HA-IRES–puro-R, pCAGGS-TRP2-HA-IRES–puro-R, and pCAGGS-hgp100-HA-IRES–puro-R. All constructs contain HA-tag or FLAG-tag except for that of GPC3 (Fig. 1A). To generate transfectant ES cell clones, B6 ES cells were transfected with the expression vectors by electroporation and selected with puromycin as described previously.[17] Transfectant ES cell clones were subjected to a differentiation culture to generate ES-DC as described previously.[24,25] ES-DC differentiated from GPC3-transfectant, SPARC-transfectant, TRP2-transfectant, or hgp100-transfectant ES cells were designated as ES-DC–GPC3, ES-DC–SPARC, ES-DC–TRP2, or ES-DC–hgp100, respectively. Recombinant mouse IL-4 was given to ES-DC at 20 hours before in vivo transfer.

### RT-PCR

Total cellular RNA was extracted by using the RNeasy Mini Kit (QIAGEN, Maryland, MD) and RT-PCR was carried out as previously described.[24] Briefly, total RNA was converted into cDNA and PCR was carried out for 30 cycles for the quantification of *GPC3*, *SPARC*, *TRP2*, *hgp100*, and glyceraldehyde-3-phosphate dehydrogenase

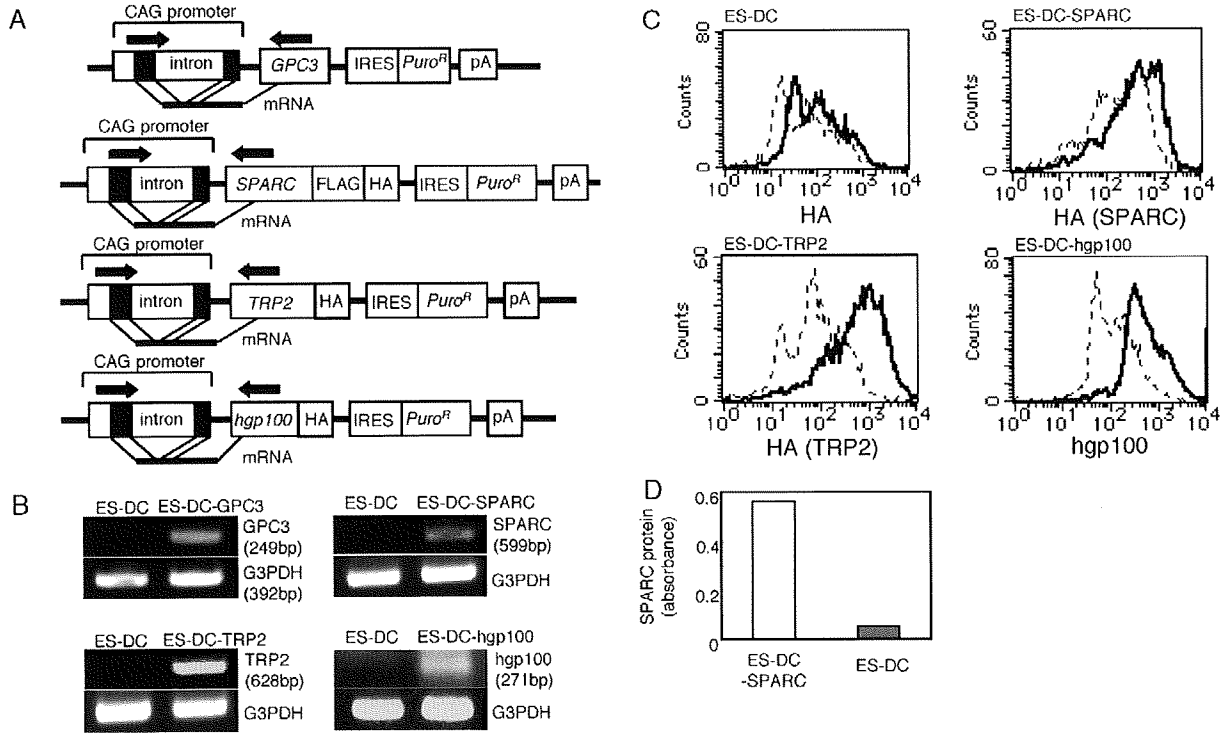


**FIGURE 1.** The generation of ES-DC expressing melanoma-associated antigens. A, Structure of vectors: pCAGGS-GPC3-IRES–puro-R, pCAGGS-SPARC-FLAG-HA-IRES–puro-R, pCAGGS-TRP2-HA-IRES–puro-R, and pCAGGS-hgp100-HA-IRES–puro-R. To obtain the vectors, each cDNA fragment encoding for a full-length of mouse *GPC3*, *SPARC*, *TRP2*, or $hgp100_{1\text{-}300}$ was inserted into a mammalian expression vector, pCAGGS-IRES–puro-R containing the CAG promoter, and an IRES–puro-R gene cassette. All constructs contain HA-tag or FLAG-tag except for that of GPC3. B, Expression of *GPC3*, *SPARC*, *TRP2*, and *hgp100* mRNA detected by RT-PCR in transfectant ES-DC. Primer sets (arrows in A) were designed to span the intron (917 bp) in the CAG promoter sequence to distinguish the PCR products of mRNA origin from the genome-integrated vector DNA origin. C, The expression of the transfected protein in ES-DC. Transfectant ES-DC were analyzed by flow cytometric analysis using intracellular staining. The staining patterns of specific antibodies (thick line) and negative control (dotted line) are shown. Anti-HA antibodies were used for staining of ES-DC, ES-DC–SPARC, and ES-DC–TRP2 and anti-hgp100 antibodies were used for staining of ES-DC–hgp100. D, SPARC protein secreted from ES-DC–SPARC or ES-DC (negative control) was measured by enzyme-linked immunosorbent assay. ES-DC indicates embryonic stem cell-derived dendritic cells; GPC3, glypican-3; hgp100, human gp100; IRES, internal ribosomal entry site; puro-R, puromycin-resistant; RT-PCR, reverse transcription polymerase chain reaction; SPARC, secreted protein acidic and rich in cysteine; TRP2, tyrosinase-related protein-2.

mRNA. The primer sequences for detection of the transgene in ES-DC and endogenous genes expressed in tumor cells are shown in Table 1. The sense strand primer used for detection of transgene-derived mRNA corresponded to the 5′ untranslated region included in the vector DNA. PCR products were visualized by ethidium bromide staining after separation by electrophoresis in a 1.5% agarose gel.

## Flow Cytometric Analysis and Enzyme-linked Immunosorbent Assay

The staining of cells and the analysis on a flow cytometer (FACScan, BD Bioscience, San Jose, CA) were performed as previously described.[24,26] The antibodies and reagents used for staining were: fluorescein isothiocyanate (FITC)-conjugated anti-HA [clone 3F10, rat immunoglobulin (Ig) G1, Fab fragments, Roche, Indianapolis, IN], rabbit anti-gp100 (AnaSpec, San Jose, CA), FITC-conjugated goat antirabbit IgG (clone ALI4408, Biosource, Camarillo, CA), antimouse CD16/CD32 (clone 2.4G2, rat IgG2b BD Bioscience), recombinant soluble dimeric mouse CD1d:Ig (BD Bioscience), phycoerythrin-conjugated antimouse IgG1 (clone A85-1, rat IgG1, BD Bioscience), mouse IgG1 isotype control (clone A111-3, mouse IgG1, BD Bioscience), FITC-conjugated antimouse T-cell receptor (TCR) β (clone H57-597, hamster IgG, BD Bioscience), and IntraPrep permeabilization reagent (Beckman Coulter, Fullerton, CA). Enzyme-linked immunosorbent assay (ELISA) was carried out as described previously.[5,10] The concentrations of HA and FLAG-tagged SPARC proteins in the culture supernatants of ES-DC were measured by ELISA in triplicate wells using anti-FLAG (clone M2; mouse IgG, SIGMA, St Louis, MO) and anti–HA-peroxidase (clone 3F10; rat IgG1, Roche).

## Induction of TAA-specific CTL and Cytotoxicity Assay

The mice were immunized intraperitoneally (IP) with each ES-DC twice with a 7-day interval. Seven days after the second immunization, spleen cells were isolated from the mice and cultured ($2.5 \times 10^6$/well) with ES-DC–GPC3, ES-DC–SPARC, ES-DC–TRP2 ($7 \times 10^4$/well), or 0.1 μM hgp100 peptide in 24-well culture plates in Roswell Park Memorial Institute-1640 supplemented with 10% horse serum, recombinant human IL-2, and 2-mercaptoethanol. After culturing for 5 days, the cells were recovered and their cytotoxic activity was analyzed by 4-hour $^{51}Cr$ release

TABLE 1. Sequences of PCR Primers

| | Sense | Antisense |
|---|---|---|
| PCR primers used for detection of transgenes expressed in ES-DC | | |
| GPC3 | 5′-CTGACTGACCGCGTTACTCCCACA-3′* | 5′-TAGCAGCATCGCCACCAGCAAGCA-3′ |
| SPARC | 5′-CTGACTGACCGCGTTACTCCCACA-3′* | 5′-GGCAAAGAAGTGGCAGGAAG-3′ |
| TRP2 | 5′-CTGACTGACCGCGTTACTCCCACA-3′* | 5′-TGGGCAGTCAGGGAATGGAT-3′ |
| hgp100 | 5′-CTGACTGACCGCGTTACTCCCACA-3′* | 5′-GCACCTATCACAGCCAAATG-3′ |
| G3PDH | 5′-GGAAAGCTGTGGCGTGATG-3′ | 5′-CTGTTGCTGTAGCCGTATTC-3′ |
| PCR primers used for detection of endogenous genes expressed in tumor cells | | |
| SPARC | 5′-ATGAGGGCCTGGATCTTCTTTCTC-3′ | 5′-TTAGATCACCAGATCCTTGTTGATGTCC-3′ |
| TRP2 | 5′-CCTTTGCGTTGCCCTACT-3′ | 5′-CTAGGCTTCCTCCGTGTATCTCTT-3′ |
| mgp100 | 5′-CCCGTGCTTGTGCTGAGTGCTCTG-3′ | 5′-ATGCTCGACCTGGACACTGGAC-3′ |

*The sense strand primer used for detection of transgene-derived mRNA corresponded to the 5′ untranslated region included in the vector DNA (Fig. 1A).
ES-DC indicates embryonic stem cell-derived dendritic cells; GPC3, glypican-3; G3PDH, glyceraldehyde-3-phosphate dehydrogenase; hgp100, human gp100; mgp100, mouse gp100; PCR, polymerase chain reaction; SPARC, secreted protein acidic and rich in cysteine; TRP2, tyrosinase-related protein-2.

assays using MCA, MCA-GPC3, B16-F10, EL-4, EL-4–SPARC, and peptide pulsed EL-4 as targets basically by the same method as described previously.[15] B16-F10 cells were pretreated with recombinant murine IFN-γ (1000 units/mL) before use as target cells as reported previously.[27]

## Subcutaneous Tumor Model

The mice were immunized IP with ES-DC–SPARC or ES-DC–TRP2 twice on days −14 and −7, and B16-F10 cells were inoculated subcutaneously into the shaved back region on day 0. In some experiments, the mice were immunized with a mixture of ES-DC–GPC3, ES-DC–SPARC, and ES-DC–TRP2. The tumor sizes were determined biweekly in a blinded fashion and the survival rate was monitored. The tumor volume was calculated as follows: tumor volume ($mm^3$) = (length × width × height).

## Measurement of Luciferase Activity

The cells or tissues were homogenized with 2 mL of lysis buffer (0.05% Triton X-100, 2 mM ethylenediaminetetraacetic acid, 0.1 M Tris, pH 7.8) and the homogenates were cleared by centrifugation at 10,000 × g for 5 minutes. Twenty-five microliter of the supernatant was mixed with 75 μL of dilution buffer (phosphate-buffered saline containing $CaCl_2$ 1.8 mM and $MgSO_4$ 0.82 mM) and 100 μL of luciferase assay buffer (Steadyliteplus, PerkinElmer, Norwalk, CT), and at 10 minutes after the mixing the light produced was measured for 1 second in a luminometer (Tristar LB941, Berthold Technologies, Bad Wildbad, Germany). The luciferase activity was converted to the number of tumor cells using a regression line ($y = 0.1134x^2 - 0.305x + 0.4213$; x = cell number, y = counts/s).

## Experimental Peritoneal Dissemination

In the preventive experiments, the mice were immunized IP with ES-DC–SPARC, ES-DC–TRP2, ES-DC–hgp100, their mixture (ES-DC–STH), or nontransfectant ES-DC twice on days 0 and 7, and B16-BL6/Luc cells were inoculated IP into mice on day 14. On day 28, the mice were euthanized and the greater omentum and pancreas were excised together and then the total luciferase activities were measured. In 1 experiment, the luciferase activities of the liver, kidney, spleen, and peritoneum were also measured. In the therapeutic experiments, B16-BL6/Luc cells were inoculated IP into mice on day 0. On days 3 and 10, ES-DC were transferred IP into mice. On day 17, mice were euthanized and luciferase activities of the greater omentum and pancreas were measured. In some experiments, ES-DC were cultured in the presence of α-GalCer (100 ng/mL) or vehicle (0.00025% Polysorbate-20) for 20 hours, and washed twice before injection. In 1 experiment, free α-GalCer (1 μg/mouse/transfer) either with or without ES-DC was transferred.

## Analysis of the Activation of NKT Cells

The activation of NKT cells in vitro was analyzed as previously described.[28] In the analysis of the activation of NKT cells in vivo, on day 0, ES-DC loaded with either α-GalCer or vehicle were transferred IP into mice. On days 1, 7, 17, or 27, the mice were euthanized and the cytotoxic activities of the whole spleen cells against Yac-1 cells were analyzed.

## In Vivo Depletion Experiments

The mice were transferred IP twice with either α-GalCer or vehicle loaded ES-DC–STH on days 0 and 7, and B16-BL6/Luc cells were inoculated IP into mice on day 14. To deplete the specific types of cells, the mice were given a total of 4 IP transfers (days −2, 5, 12, and 19) of monoclonal antibodies (mAbs), ascites (0.1 mL/mouse/transfer) from hybridoma-bearing nude mice, or polyclonal rabbit antiasialo GM1 antibody (Wako, Tokyo, Japan; 20 μL/mouse/transfer). The mAbs used were rat antimouse CD4 mAb (clone GK1.5) and rat antimouse CD8 mAb (clone 2.43). Normal rat IgG (Sigma-Aldrich, St Louis, MO; 200 μg/mouse/transfer) was used as a control. The depletion of specific cell subsets by treatment with antibodies was confirmed by a flow cytometric analysis of spleen cells, which showed a > 90% specific depletion.

## Spontaneous Metastasis Experiments

In the preventive experiments, α-GalCer–loaded ES-DC or ES-DC–STH were transferred IP into mice twice on days 0 and 7. On day 14, the footpad of mice was inoculated with B16-BL6/Luc cells. On day 35, mice were euthanized, the lungs were excised, and total luciferase activities were measured. In the therapeutic experiments, B16-BL6/Luc cells were inoculated into the footpad on day 0. On days 3 and 10, ES-DC were transferred IP into mice. On day 21, mice were euthanized and luciferase activities of the inguinal lymph nodes were measured.

## Statistical Analysis

Two-tailed Student *t* test was used to determine the statistical significance of differences in the tumor growth

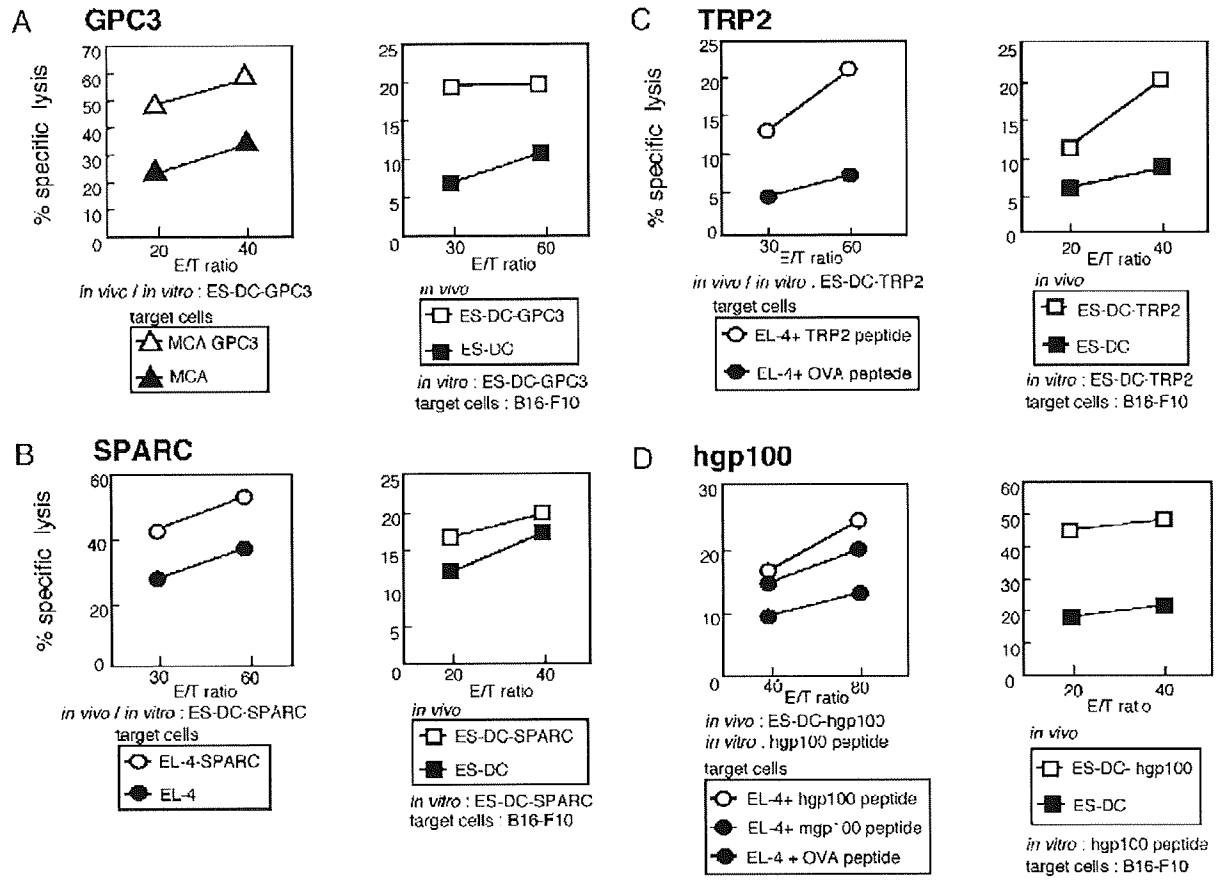


**FIGURE 2.** The priming of antigen-specific CTL in vivo with ES-DC expressing tumor-associated antigen. The mice were immunized intraperitoneally twice with each $1 \times 10^5$ ES-DC (as indicated in figure) on days 0 and 7. On day 14, spleen cells were isolated and cultured with $1 \times 10^5$ ES-DC–GPC3, ES-DC–SPARC, ES-DC–TRP2, or 0.1 μM human gp100 peptide per well in the presence of rhIL-2 (100 units/mL) for 5 days. Four-hour $^{51}Cr$ release assays were carried out using the obtained resultant cells to evaluate the capacity to kill MCA and MCA-GPC3 (A; left), EL-4 and EL-4–SPARC (B; left), EL-4 pulsed with the epitope peptide of TRP2 (C; left) and human or mouse gp100 (D; left), or B16-F10 (A–D; right). The results are expressed as percentage specific lysis from triplicate assays. The data are each representative of 2 independent experiments with similar results. CTL indicates cytotoxic T lymphocytes; ES-DC, embryonic stem cell-derived dendritic cells; GPC3, glypican-3; rhIL, recombinant human interleukin; SPARC, secreted protein acidic and rich in cysteine; TRP2, tyrosinase-related protein-2.

between the treatment groups. The Kaplan-Meier analysis with the Breslow-Gehan-Wilcoxon test was used to determine that of survival. The Mann-Whitney $U$ test was used to examine the differences of luciferase activities. $P < 0.05$ was considered to be significant. Statistical analyses were performed by using the StatView 5.0 software package (Abacus Concepts, Calabasas, CA).

## RESULTS

### Generation of ES-DC expressing Melanoma Antigens

B6 ES cells were transfected with the *GPC3*, *SPARC*, *TRP2*, and *hgp100* expression vectors; pCAGGS-GPC3-IRES–puro-R, pCAGGS-SPARC-FLAG-HA-IRES–puro-R, pCAGGS-TRP2-HA-IRES–puro-R, pCAGGS-hgp100-HA-IRES–puro-R (Fig. 1A), and several transfectant clones were isolated. The transfectant ES cell clones were subjected to differentiation to ES-DC, and the transfectant clone expressing the highest level of each TAA was selected on the basis of the RT-PCR, fluorescence-activated cell sorting analysis, and ELISA (Fig. 1B–D).

### Priming of TAA-specific CTL With Genetically Modified ES-DC

The capacity of ES-DC–GPC3, ES-DC–SPARC, ES-DC–TRP2, and ES-DC–hgp100 to prime each TAA-specific CTL was analyzed. Other investigators reported that immunization of mice with hgp100 elicited a mouse gp100-specific $CD8^+$ T-cell response more efficiently than that with mouse gp100.[29] Therefore, ES-DC expressing hgp100 were generated in the present study. The mice were immunized with ES-DC–GPC3, ES-DC–SPARC, ES-DC–TRP2, ES-DC–hgp100, or nontransfectant ES-DC, respectively, on days 0 and 7. On day 14, the spleen cells were isolated and cultured with ES-DC–GPC3, ES-DC–SPARC, ES-DC–TRP2, or hgp100 peptide for 5 days. Next, the cells were recovered and their TAA-specific killing activities were analyzed. For the analysis of GPC3-specific and SPARC-specific CTL, MCA-GPC3 and EL-4–SPARC were used as targets. For TRP2-specific and gp100-specific CTL, EL-4 cells pulsed with previously

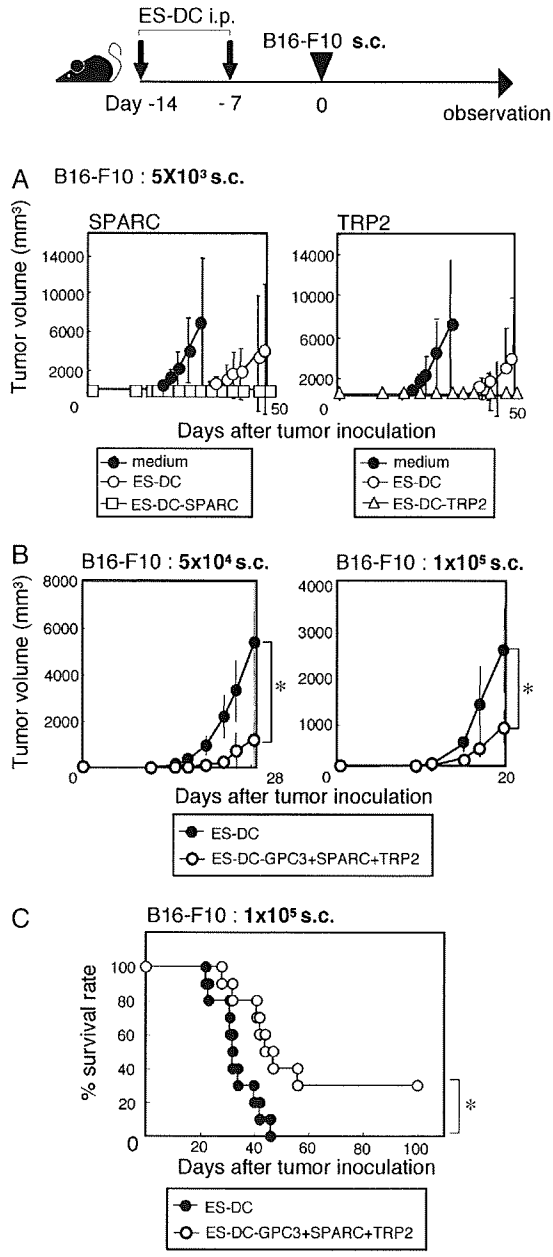


**FIGURE 3.** Protection against a subcutaneously inoculated tumor. A, About $1 \times 10^5$ ES-DC–SPARC or ES-DC–TRP2 were transferred IP into mice twice on days $-14$ and $-7$, and $5 \times 10^3$ B16-F10 cells were inoculated subcutaneously into the shaved back region on day 0. B, About $3 \times 10^5$ of nontransfectant ES-DC (control) or a mixture of ES-DC–GPC3, ES-DC–SPARC, and ES-DC–TRP2 that consisted of $1 \times 10^5$ of each ES-DC was transferred IP, and $5 \times 10^4$ or $1 \times 10^5$ B16-F10 cells were inoculated in the same schedule as above. The tumor sizes were determined biweekly in a blinded fashion and the survival rate was monitored (C). The tumor volume was calculated as follows: tumor volume ($mm^3$) = (length × width × height). The data are the mean ± SD (A–C, n = 5; D, n = 10; *$P$<0.05). The data are each representative of 2 independent experiments with similar results. ES-DC indicates embryonic stem cell-derived dendritic cells; GPC3, glypican-3; IP, intraperitoneal; SPARC, secreted protein acidic and rich in cysteine; TRP2, tyrosinase-related protein-2.

reported dominant epitopes of TRP2 and gp100 we used. As shown in Fig. 2A–D; left, the effector cells primed with ES-DC–GPC3, ES-DC–SPARC, ES-DC–TRP2, or ES-DC–hgp100 exhibited significantly higher killing activities against the target cells that specifically express each TAA. Furthermore, the effector cells activated with each TAA-expressing ES-DC in vivo showed significantly higher killing activities against the B16-F10 that naturally express each TAA (Fig. 2A–D; right). In contrast, spleen cells isolated from mice transferred with nontransfectant ES-DC and cocultured in vitro with each TAA exhibited a basal level killing activity. These results suggest that ES-DC–GPC3, ES-DC–SPARC, ES-DC–TRP2, and ES-DC–hgp100 have the capacity to prime TAA-specific CTL in vivo.

## Protection Against Subcutaneously Inoculated Tumor

ES-DC–GPC3 can induce an antigen-specific protective effect against $5 \times 10^3$ subcutaneously inoculated B16-F10 cells naturally expressing GPC3.[15] However, the anticancer effect was insufficient when the mice were challenged with a larger number ($1 \times 10^4$) of melanoma cells (unpublished observation). The present study examined whether ES-DC–SPARC or ES-DC–TRP2 could protect the recipient mice from a subcutaneous inoculation of $5 \times 10^3$ B16-F10 cells. Figure 3A shows that immunization with ES-DC–SPARC or ES-DC–TRP2 provided complete protection against $5 \times 10^3$ B16-F10 inoculations. We observed a certain antitumor effect of nontransfectant ES-DC (Fig. 3A). This phenomenon may be owing to the fact that even nontransfectant ES-DC produced cytokines with an antitumor effect, such as IL-12 and tumor necrosis factor-α. In addition, nontransfectant ES-DC may have presented tumor cell-derived TAA and activated specific CTL, as intrinsic natural DC did. However, the TAA-specific effect elicited by these ES-DC was not significant when the mice were inoculated with $5 \times 10^4$ B16-F10 cells (unpublished observation). Collectively, ES-DC expressing single TAA could protect the mice from subcutaneous challenge with a relatively small number of tumor cells, however, the effect was insufficient to protect the mice from a challenge with a larger number of tumor cells.

The simultaneous in vivo transfer of ES-DC–GPC3, ES-DC–SPARC, and ES-DC–TRP2 might protect the recipient mice from a challenge with a relatively large number of B16-F10 cells. Figure 3B demonstrates the transfer of a combination of these TAA-transfectant ES-DC to elicit a significant protection against inoculation with $5 \times 10^4$ and $1 \times 10^5$ B16-F10 cells, thus resulting in a significant prolongation of the survival time of the treated mice (Fig. 3C). Therefore, immunotherapy with multiple TAA is more effective than that with a single TAA.

## Prevention of Peritoneal Dissemination of Melanoma by Preimmunization With Multiple TAA-targeted ES-DC

Experiments on preventing the growth of tumors inoculated subcutaneously are often performed and they are convenient models to observe the effects of cancer immunotherapy, but they do not accurately reflect clinical situations. In a preclinical study of cancer immunotherapy, it is important to examine in the metastatic models that are resistant to cancer immunotherapy. Therefore, the effects

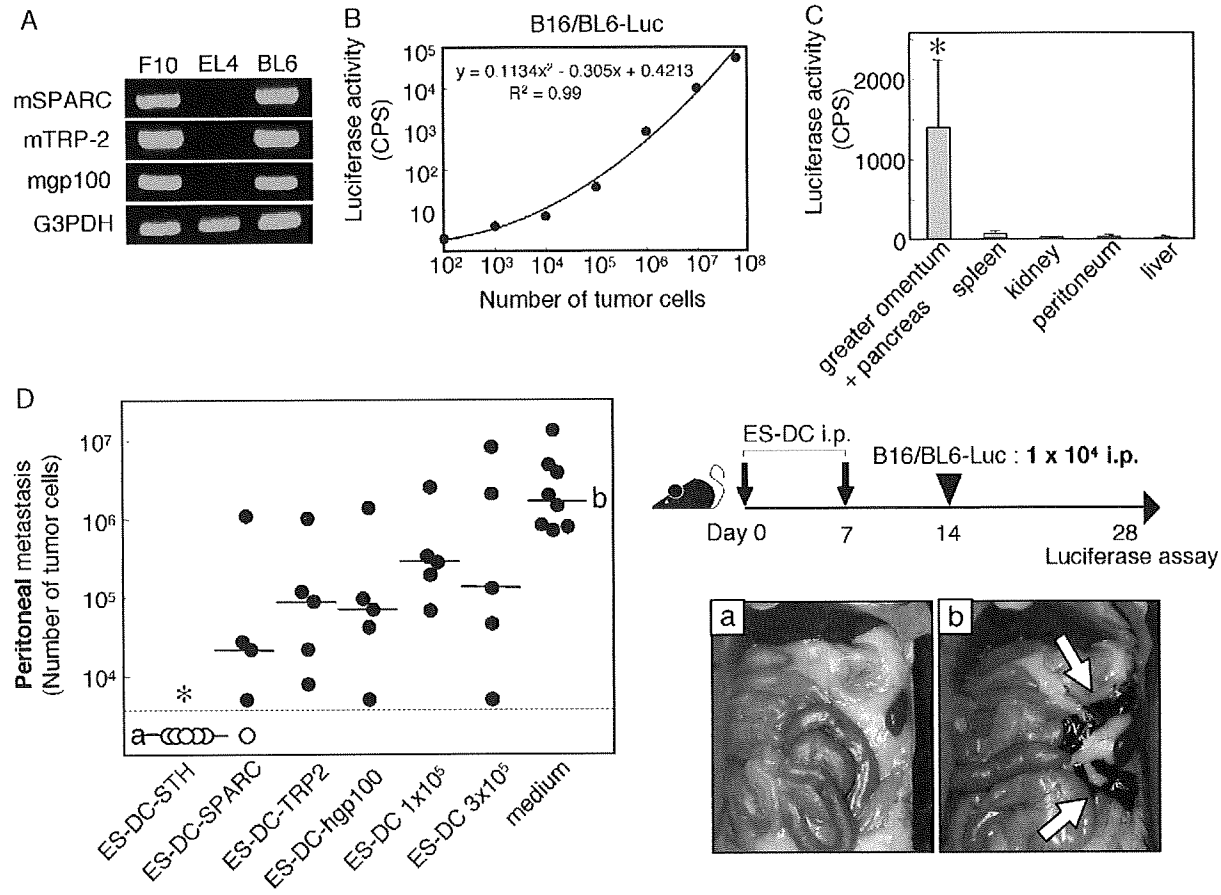


**FIGURE 4.** The prevention of peritoneal dissemination of melanoma by multiple tumor-associated antigen-targeted immunization with ES-DC. A, The expressions of SPARC, TRP2, and mouse gp100 mRNA in B16-BL6 were detected by RT-PCR. B, Luciferase activities in the homogenates of B16-BL6/Luc cells at the indicated numbers are shown. C, Luciferase activity of the homogenate of organs isolated on 17 days after IP inoculation of $1 \times 10^4$ B16-BL6/Luc cells. The data are shown as the counts per second (CPS). D, ES-DC–SPARC ($1 \times 10^5$ cells), ES-DC–TRP2 ($1 \times 10^5$ cells), ES-DC–hgp100 ($1 \times 10^5$ cells), nontransfectant ES-DC ($1 \times 10^5$ cells), nontransfectant ES-DC ($3 \times 10^5$ cells), or a equal mixture of ES-DC–SPARC, ES-DC–TRP2, and ES-DC–hgp100 (ES-DC–STH; $3 \times 10^5$ cells in total) were inoculated IP into mice twice on days 0 and 7, and $1 \times 10^4$ B16-BL6/Luc cells were inoculated IP into mice on day 14. Mice were euthanized on day 28. The greater omentum and pancreas were excised together and the total luciferase activity was measured. The luciferase activity was converted to the number of tumor cells using a regression line shown in B. Typical examples of peritoneal dissemination of B16-BL6/Luc cells are shown in mice inoculated with (left; A) ES-DC–STH or (right; B) medium (C, n = 5; D, n = 5 to 8; $*P<0.05$). Dotted line indicates the detection limit. The data are each representative of 2 independent experiments with similar results. ES-DC indicates embryonic stem cell-derived dendritic cells; IP indicates intraperitoneal; RT-PCR, reverse transcription polymerase chain reaction; SPARC, secreted protein acidic and rich in cysteine; TRP2, tyrosinase-related protein-2.

of ES-DC were evaluated in the peritoneal dissemination model.[18,28] Previously, the survival rate was the only end point in the peritoneal dissemination model. To evaluate tumor metastasis, labeling of cells by introducing reporter gene is a promising technique because the metastatic cells can be quantified. A firefly luciferase gene was introduced into a mouse melanoma B16-BL6 cell line that is a highly metastatic subline of B16, as previously described[30] and established a transfectant clone B16-BL6/Luc. The expressions of *SPARC*, *TRP2*, and mouse *gp100* mRNA were detected by RT-PCR analysis in B16-BL6 (Fig. 4A) and *gpc3* mRNA was not detected (unpublished observation). The luciferase activities in the homogenates of B16-BL6/Luc cells indicated that the luciferase activity was correlated with the number of B16-BL6/Luc cells at least in the range from 7 to 60,000 counts/s (Fig. 4B). The luciferase activity of the homogenate of each organ was confirmed on day 17 after IP inoculation of $1 \times 10^4$ B16-BL6/Luc cells (Fig. 4C). As others have reported, the greater omentum and pancreas were the most common site of metastasis in the early stage of peritoneal dissemination.[31] Because the luciferase activities of the greater omentum and pancreas were significantly higher than other organs such as the spleen, liver, kidney, and peritoneum, the luciferase activities of greater omentum and pancreas were measured to evaluate the metastasis of abdominal organs in the subsequent experiments.

The preventive effects of ES-DC were evaluated in the peritoneal tumor dissemination model (Fig. 4D). Immunization with ES-DC–SPARC, ES-DC–TRP2, or ES-DC–hgp100 did not show a TAA-specific, antitumor effect to inhibit the dissemination when $1 \times 10^4$ B16-BL6/Luc cells were inoculated. However, simultaneous in vivo transfer of ES-DC–SPARC, ES-DC–TRP2, and ES-DC–hgp100 completely prevented the tumor dissemination.

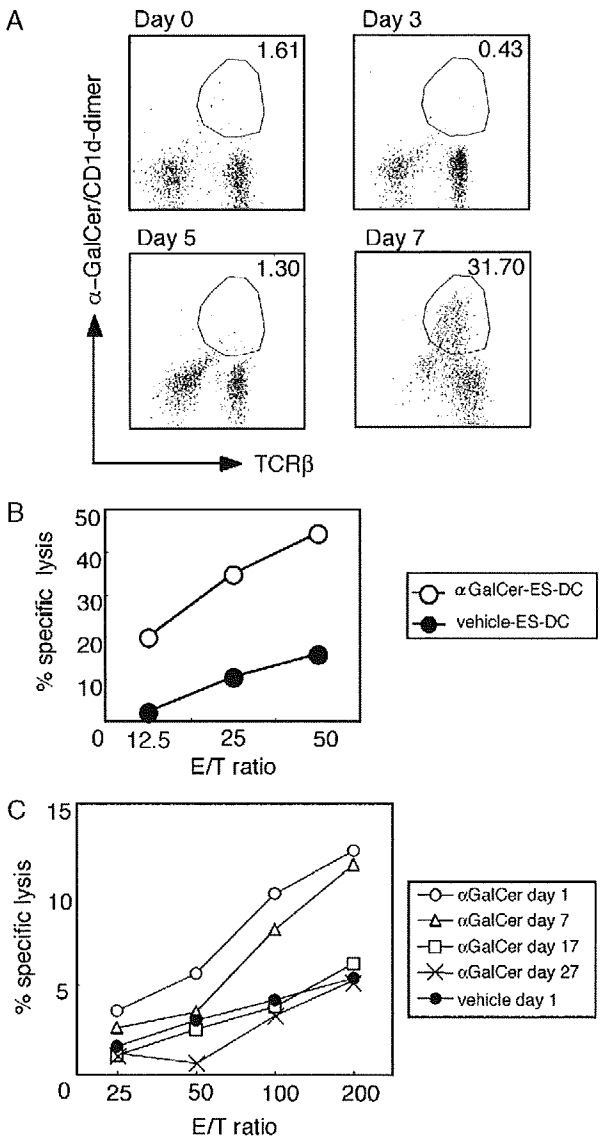


**FIGURE 5.** The activation of NKT cells by α-GalCer–loaded ES-DC. A, ES-DC were cultured in the presence of α-GalCer or vehicle alone for 20 hours, washed twice, and cocultured with splenic T cells of syngeneic mice ($5 \times 10^4$ DC+$2.5 \times 10^6$ T cells/well in 24-well culture plate). On day 0, 3, 5, or 7, the cells were analyzed by flow cytometric analysis. The percentage of NKT cells, defined as TCRβ$^+$ and α-GalCer/CD1d dimer reactive cells, is indicated. B, On day 5, the effecter cells recovered from the culture were analyzed for their cytotoxic activities by a 4-hour $^{51}$Cr-release assay using Yac-1 cells as target cells ($1 \times 10^4$ cells/well) at the indicated effecter:target ratio. C, In vivo activation of NKT cells by α-GalCer–loaded ES-DC. On day 0, ES-DC loaded with either α-GalCer or vehicle alone were transferred intraperitoneally into mice ($1 \times 10^6$ cells/mouse). On day 1, 7, 17, or 27, the mice were euthanized and the cytotoxic activities of whole spleen cells against Yac-1 cells were analyzed, as described above. The results are expressed as percentage specific lysis from triplicate assays. ES-DC indicates embryonic stem cell-derived dendritic cells; NKT, natural killer T; TCR, T-cell receptor; α-GalCer, α-galactosylceramide.

Therefore, the potency of immunotherapy with multiple TAA was confirmed also in the peritoneal dissemination model.

## Activation of NKT Cells by α-GalCer–loaded ES-DC

Others have reported that α-GalCer loaded on mature DC induced more prolonged IFN-γ production by NKT cells and better protection against B16 melanoma than free α-GalCer.[20] The capacity of ES-DC was first confirmed to activate NKT cells in vitro. As shown in Figure 5A, NKT cells detected by α-GalCer/CD1d dimer represented 1.61% of splenic T cells before stimulation with α-GalCer–loaded ES-DC (day 0). After stimulation, TCRβ$^+$ dimer$^+$ cells almost disappeared on day 3, probably reflecting activation-induced down-regulation of the surface TCR.[32,33] This population began to reappear on day 5 and was dramatically increased (31.7%) on day 7, consistent with previous reports that activated NKT cells remain quiescent for a while, but eventually proliferate. The cultured cells recovered on day 5 exhibited strong cytotoxic activities against Yac-1 cells (Fig. 5B). These results indicate that α-GalCer–loaded ES-DC induced significant activation and of NKT cells in vitro. Next, the duration of activation of NKT cells induced by ES-DC was analyzed in vivo. On day 0, ES-DC loaded with either α-GalCer or vehicle were injected IP into mice. On days 1, 7, 17, or 27, the mice were euthanized and the cytotoxic activity of whole spleen cells against Yac-1 cells was analyzed. Figure 5C showed the Yac-1 cell-killing activities of spleen cells reflecting activation of NKT cells. The killing activities sustained for 1 week, and after 2 weeks the effect decreased to the background level.

## Potent Anticancer Effects of Multiple TAA-targeted ES-DC Loaded With α-GalCer

We evaluated the effects of multiple TAA-targeted and α-GalCer–loaded ES-DC in several metastatic models. As shown in Figure 6A, simultaneous in vivo transfer of vehicle-loaded ES-DC–SPARC, ES-DC–TRP2, and ES-DC–hgp100 did not show a significant inhibition of the dissemination of $5 \times 10^4$ B16-BL6/Luc cells, when 5 times more cells were injected IP in comparison with the experiments shown in Figure 4D. Although α-GalCer–loaded ES-DC without TAA induced a significant but a partial protection, a mixture of 3 kinds of TAA-transfectant ES-DC loaded with α-GalCer completely protected the mice from tumor dissemination. As shown in Figure 6B, α-GalCer–loaded ES-DC expressing TAA induced a significantly more potent protection than either 1 μg of free α-GalCer alone (the commonly used dose) or that injected simultaneously with ES-DC expressing TAA. These results clearly indicate the advantage of loading α-GalCer to DC to improve the anticancer effects. To analyze the effector cell populations induced by α-GalCer–loaded ES-DC with TAA, in vivo depletion of CD4$^+$T, CD8$^+$T, or natural killer (NK) cells with specific antibodies was performed as shown in Figure 6C. The preventive effects of the immunization with α-GalCer–loaded TAA-expressing DC (compared with vehicle-loaded TAA-expressing DC) were almost totally abrogated when CD4$^+$T cells, CD8$^+$T cells, or NK cells were depleted. These results suggest that all of 3 effector cell subsets were essential to achieve the protective effect.

Spontaneous pulmonary metastasis was induced by inoculation of B16-BL6/Luc cells into the footpad as previously described.[34] The mixture of α-GalCer–loaded ES-DC–SPARC, ES-DC–TRP2, and ES-DC–hgp100 or α-GalCer–loaded ES-DC without TAA were transferred

IP into mice twice on days 0 and 7. On day 14, $2 \times 10^6$ B16-BL6/Luc cells were inoculated into the footpad of mice. On day 35, the mice were euthanized, the lungs were excised, and luciferase activities were measured. As shown in Figure 7A, in vivo transfer of a mixture of 3 kinds of TAA-transfectant ES-DC loaded with α-GalCer induced significant protection compared with α-GalCer–loaded ES-DC without TAA also in the spontaneous pulmonary metastasis model. In this model, we have no evidence indicating that the loading of α-GalCer to TAA-expressing ES-DC provided any benefit in regard to inhibiting the local tumor growth in the primary lesion. This result may be owing to the tissue distribution of NKT cells. NKT cells are known to mainly localize in the liver, lung, spleen, bone marrow, and peritoneal cavity.

Finally, the effects of the in vivo transfer of a mixture of 3 kinds of TAA-transfectant ES-DC loaded with α-GalCer in the therapeutic setting on lymph node metastasis and peritoneal dissemination were evaluated. On day 0, $2 \times 10^6$ B16-BL6/Luc cells were inoculated into the footpad or $1 \times 10^4$ tumor cells were inoculated IP into mice. On days 3 and 10, ES-DC were transferred IP, and on day 21 or 17, respectively, the mice were euthanized and luciferase activities were measured. Multiple TAA-targeted ES-DC loaded with α-GalCer induced significant therapeutic effects compared with α-GalCer–loaded ES-DC without TAA in the model of spontaneous metastasis to inguinal lymph node (Fig. 7B). As shown in Figure 7C, although the in vivo transfer of α-GalCer–loaded ES-DC without TAA or vehicle-loaded ES-DC with TAA showed insufficient effects, a mixture of 3 kinds of TAA-transfectant ES-DC loaded with α-GalCer induced a significant therapeutic effect in the peritoneal dissemination model.

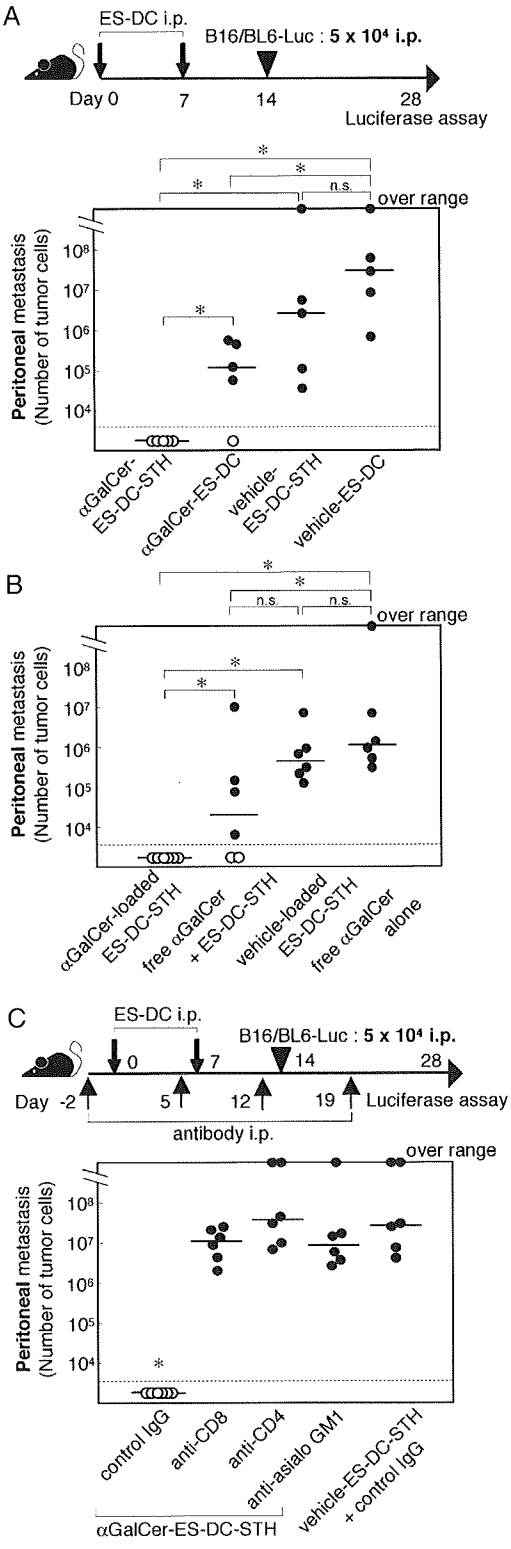


**FIGURE 6.** Preventive anticancer effects of multiple tumor-associated antigen-targeted vaccinations with α-GalCer–loaded ES-DC. A, The mixture of ES-DC–SPARC, ES-DC–TRP2, and ES-DC–hgp100 ($3 \times 10^5$) loaded with either α-GalCer (αGalCer–ES-DC–STH) or vehicle (vehicle–ES-DC–STH) or nontransfectant ES-DC loaded with either α-GalCer (α-GalCer–ES-DC) or vehicle (vehicle–ES-DC) were transferred IP into mice twice on days 0 and 7, and $5 \times 10^4$ B16-BL6/Luc cells were inoculated IP into mice on day 14. On day 28, the mice were euthanized and the greater omentum and pancreas were excised together and the total luciferase activities were measured. B, $3 \times 10^5$ α-GalCer–loaded ES-DC–STH, free α-GalCer (1 μg/mouse/transfer) combined with ES-DC–STH, vehicle-loaded ES-DC–STH, and free α-GalCer alone (1 μg/mouse/transfer) were transferred IP into mice twice on days 0 and 7. About $5 \times 10^4$ B16-BL6/Luc cells were inoculated and luciferase activities were measured using the same protocol as A. C, $CD4^+$ T, $CD8^+$ T, or NK cells were depleted in vivo by the IP transfer of anti-CD4 mAb, anti-CD8 mAb, or polyclonal rabbit anti-asialo GM1 Ab. During this procedure, the mice were immunized with α-GalCer–loaded or vehicle-loaded ES-DC–STH and challenged IP with B16-BL6/Luc cells in the same protocol as A. Dotted line indicates the detection limit (A, n = 5; B and C, n = 6; *$P<0.05$). The data are each representative of 2 independent experiments with similar results. ES-DC indicates embryonic stem cell-derived dendritic cells; hgp100, human gp100; IP, intraperitoneal; mAb, monoclonal antibody; NK, natural killer; SPARC, secreted protein acidic and rich in cysteine; TRP2, tyrosinase-related protein-2; α-GalCer, α-galactosylceramide.

## DISCUSSION

The anticancer effects of multiple TAA-targeted immunotherapies against mouse melanoma were evaluated by using α-GalCer–loaded and genetically engineered ES-DC. Four TAA that were naturally overexpressed in melanoma were selected, GPC3, SPARC, TRP2, and gp100. SPARC is expressed in various types of cancer tissues[35,36] and implicated in evasion of cancers from

immune attack.[37,38] The present study is the first to demonstrate that SPARC can be a target antigen for cancer immunotherapy. Figures 2B, 3A and 4D show that the effect of SPARC as the target antigen was comparable with the previously known melanoma-associated antigen, TRP2, or gp100.

CTL specific to each TAA were sensitized by the in vivo transfer of DC transfected with *GPC3*, *SPARC*, *TRP2*, or *hgp100* gene. However, the anticancer effects of ES-DC expressing single TAA in vivo were insufficient (Fig. 4D). These results are quite similar to the situation of recent T cell-targeted cancer immunotherapy. Using DC expressing multiple TAA for cancer immunotherapy makes sense and several studies have been reported.[39–41] However, there are very few reports that directly demonstrate the advantage of multiple as compared with single TAA-targeted immunotherapy.[42] As shown in Figures 3B, C and 4D, preimmunization with the mixture of 3 independent TAA transfectant ES-DC protected the mice more efficiently than the ES-DC expressing single TAA. The enhancement of antitumor immunity by the transfer of a mixture of 3 kinds of TAA-transfectant DC could be owing to an increase of number of CTL attacking tumor cells and a low frequency of immune escape.

In the past decade, α-GalCer has been attracting attention as a novel immunostimulatory reagent for cancer immunotherapy. CD1d is monomorphic and thus CD1d–α-GalCer–complex on DC can stimulate the NKT cells of any recipients. On the basis of the promising results of preclinical studies demonstrating the anticancer effects of α-GalCer–loaded DC,[20] several phase 1 clinical studies have been conducted. Although the activation and expansion of NKT cells by the administration of α-GalCer–loaded DC has been observed, the results seemed to be unsatisfactory from the viewpoint of the clinical effects.[43–46] The present study evaluated the effects of loading α-GalCer onto ES-DC–expressing endogenous TAA to induce anticancer immunity. Upon loading with α-GalCer, ES-DC had a capacity to activate NKT cells (Fig. 5). Figure 5C showed that the killing activity induced by the in vivo administration of α-GalCer–loaded ES-DC through the activation of NKT cells was sustained 1 week, and after 2 weeks the effect decreased to the background level. Despite this transient NKT cell activating capacity of α-GalCer–loaded ES-DC, anticancer effects induced by a mixture of 3 kinds of TAA-transfectant ES-DC loaded with α-GalCer showed a potent effect on inhibiting the growth of B16-BL6/Luc at 2 or 5 weeks after the administration as shown in Figures 6

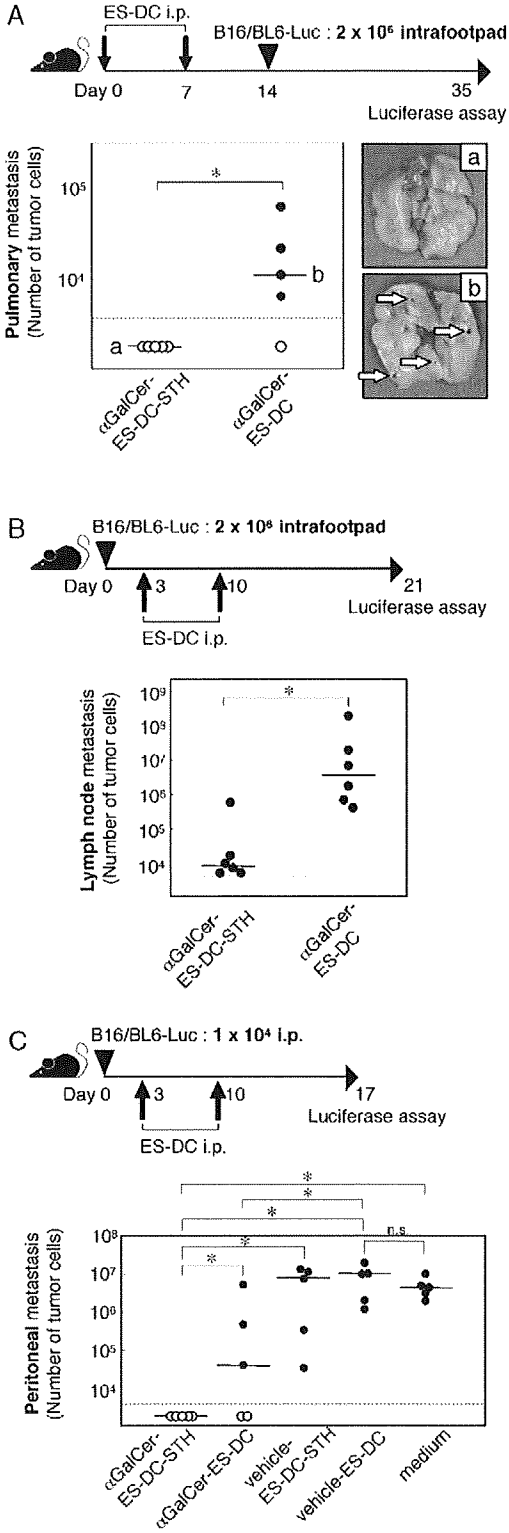


**FIGURE 7.** Potent anticancer effects of multiple tumor-associated antigen-targeted vaccinations with α-GalCer-loaded ES-DC. A, About $3 \times 10^5$ of α-GalCer–ES-DC–STH or α-GalCer–ES-DC were transferred IP into mice twice on days 0 and 7. On day 14, $2 \times 10^6$ B16-BL6/Luc cells were inoculated into the footpad of mice. On day 35, the mice were euthanized, the lungs were excised, and luciferase activities were measured. Typical examples of pulmonary metastasis of B16-BL6/Luc cells in mice are shown: above; A, α-GalCer–ES-DC–STH; below; B, α-GalCer–ES-DC. B, On day 0, $2 \times 10^6$ B16-BL6/Luc cells were inoculated into the footpad of mice. On days 3 and 10, each ES-DC was transferred IP. On day 21, the mice were euthanized and the luciferase activities of the inguinal lymph nodes were measured. C, On day 0, $1 \times 10^4$ B16-BL6/Luc cells were inoculated IP into mice. On days 3 and 10, each ES-DC was transferred IP. On day 17, the mice were euthanized and the luciferase activities of the greater omentum and pancreas were measured. Dotted line indicates the detection limit (A and C, n = 5; B, n = 6; *$P$<0.05). The data are each representative of 2 independent experiments with similar results. ES-DC indicates embryonic stem cell-derived dendritic cells; IP, intraperitoneal; α-GalCer, α-galactosylceramide.

and 7. In contrast, α-GalCer–loaded ES-DC without TAA showed an insufficient effect under the same conditions. This suggests that α-GalCer–loaded ES-DC have potent, antigen nonspecific effect in the early phase after administration, but sustained anticancer effect requires activation of TAA-specific CTL induced by ES-DC expressing TAA. Interestingly, the others reported that NKT cells activation induced by α-GalCer–loaded mature DC helped to boost adaptive immunity in vivo.[45] We performed an IFN-γ enzyme-linked immunosorbent spot assay to investigate whether the loading of α-GalCer to TAA-expressing DC would enhance the TAA-specific immunoresponse. However, no significant enhancement was observed when the mice were immunized with α-GalCer–loaded TAA-expressing DC in comparison with the vehicle-loaded TAA-expressing DC (unpublished observation). The preventive effects of the immunization with α-GalCer–loaded TAA-expressing DC (compared with vehicle-loaded TAA-expressing DC) were almost totally abrogated when the $CD4^+$ T cells, $CD8^+$ T cells, or NK cells were depleted (Fig. 6C). Collectively, we considered that the enhanced antitumor effects induced by α-GalCer–loaded TAA-expressing DC came from the cooperative work of $CD4^+$ T cells, $CD8^+$ T cells, and NK cells.

Anticancer immunotherapy with DC loaded with human leukocyte antigen (HLA)-binding peptides derived from TAA has been tested clinically in many institutions. In most cases, the DC are generated by culture of monocytes obtained from peripheral blood of the patients. To generate a sufficient number of DC for treatment, apheresis, a procedure that is sometimes invasive for patients with advanced stages of cancer, is necessary. In addition, the culture to generate DC should be carried out separately for each patient and treatment, and thus the procedure used at present may be too labor-intensive and expensive to be applied broadly in a practical setting. Alternately, the source of ES-DC, ES cells, has the capacity to propagate infinitely and multiple gene-transfectant ES-DC can be generated by the sequential transfection of ES cells with vectors bearing different selection markers.[18,24,25] Generation and genetic modification of ES-DC from human ES cells is achieved by the currently established method.[47] It may, therefore, be possible to generate multiple gene-transfectant human ES-DC expressing TAA plus immunostimulating molecules, which could thus more potently stimulate anticancer immunity than monocyte-derived DC do.

Considering the future clinical application of ES-DC, allogenicity (ie, differences in the genetic background) between patients to be treated and ES cells as a source for DC may cause problems. However, it is expected that human ES cells sharing some HLA alleles with the patients will be available for most cases. Mouse ES-DC administered into semiallogenic recipients, sharing 1 major histocompatibility complex (MHC) haplotype with the ES-DC, effectively primed antigen-specific CTL, thus suggesting that ES-DC can survive for a sufficient period to stimulate antigen-specific CTL restricted by the shared MHC class I.[48] However, in the same semiallogenic setting, the 5 times injection of nonantigen-loaded ES-DC significantly reduced the efficiency of priming of antigen-specific CTL induced by the subsequent injection of antigen-loaded ES-DC (unpublished observation). Therefore, repetitive stimulation with ES-DC expressing allogenic MHC may result in activation and expansion of allogenic MHC class I-reactive CTL, and in such recipients subsequently transferred ES-DC may be rapidly eliminated. Repeated immunization may be required in clinical applications to induce strong anticancer immunity. Therefore, the problem of the histoincompatibility between ES cell lines and recipients should be resolved. The methods for targeted gene modification of human ES cells and for targeted chromosome elimination of mouse ES cells have been developed. To overcome the problem of histoincompatibility, genetic modification to inhibit expression of endogenous HLA class I in ES-DC may be effective. A disruption of the genes for the molecules necessary for the cell surface expression of HLA class I molecules, such as transporter associated with antigen processing or β2-microglobulin (β2M), is presumably feasible. Along this line, we recently reported that the efficient activation of antigen-specific CTL was induced by TAP1 or β2M disrupted and recipient-matched MHC class I introduced mouse ES-DC.[19] We are now preparing to introduce expression vector encoding for β2M-linked form of recipient-matched HLA class I heavy chain into TAP1-deficient or β2M-deficient human ES cells.

Previous studies on ES-DC were performed by using well-established TT2 ES cells.[15,18,28] The present study confirmed that ES-DC could be generated from B6 ES cells with the same method previously established by using TT2 ES cells.[17] ES-DC generated from B6 ES cells were comparable with TT2 ES cells in differentiation, proliferation, surface phenotype, and antigen presentation. In addition, ES-DC could be generated from other ES cell lines (unpublished observation), thus suggesting that the method to generate ES-DC can be applied to various types of mouse ES cells.

Other studies have reported the generation of induced pluripotent stem (iPS) cells from adult human dermal fibroblasts with the defined 4 factors: Oct3/4, Sox2, Klf4, and c-Myc.[49] Human iPS cells are similar to human ES cells in morphology, proliferation, surface antigens, gene expression, epigenetic status of pluripotent cell-specific genes, and telomerase activity. DC can be generated from mouse iPS cells (unpublished observation) and testing is underway to determine whether DC could be generated from human iPS cells. Tailor-made medicine may, therefore, someday be possible if "iPS-DC" can be generated in the future.

## ACKNOWLEDGMENTS

*The authors thank Drs H. Suemori and N. Nakatsuji for B6, Dr M. Nishikawa for pCMV-Luc, and Kirin Brewery for α-GalCer.*

## REFERENCES

1. Rosenberg SA, Yang JC, Restifo NP. Cancer immunotherapy: moving beyond current vaccines. *Nat Med.* 2004;10:909–915.
2. Finke LH, Wentworth K, Blumenstein B, et al. Lessons from randomized phase III studies with active cancer immunotherapies—outcomes from the 2006 meeting of the Cancer Vaccine Consortium (CVC). *Vaccine.* 2007;25(suppl 2):B97–B109.
3. Ostrand-Rosenberg S. Animal models of tumor immunity, immunotherapy and cancer vaccines. *Curr Opin Immunol.* 2004;16:143–150.
4. Kageshita T, Ishihara T, Campoli M, et al. Selective monomorphic and polymorphic HLA class I antigenic determinant loss in surgically removed melanoma lesions. *Tissue Antigens.* 2005;65:419–428.
5. Nakatsura T, Yoshitake Y, Senju S, et al. Glypican-3, overexpressed specifically in human hepatocellular carcinoma,

is a novel tumor marker. *Biochem Biophys Res Commun.* 2003;306:16–25.
6. Nakatsura T, Komori H, Kubo T, et al. Mouse homologue of a novel human oncofetal antigen, glypican-3, evokes T-cell-mediated tumor rejection without autoimmune reactions in mice. *Clin Cancer Res.* 2004;10:8630–8640.
7. Komori H, Nakatsura T, Senju S, et al. Identification of HLA-A2- or HLA-A24-restricted CTL epitopes possibly useful for glypican-3-specific immunotherapy of hepatocellular carcinoma. *Clin Cancer Res.* 2006;12:2689–2697.
8. Lane TF, Sage EH. The biology of SPARC, a protein that modulates cell-matrix interactions. *FASEB J.* 1994;8:163–173.
9. Nakatsura T, Kageshita T, Ito S, et al. Identification of glypican-3 as a novel tumor marker for melanoma. *Clin Cancer Res.* 2004;10:6612–6621.
10. Ikuta Y, Nakatsura T, Kageshita T, et al. Highly sensitive detection of melanoma at an early stage based on the increased serum secreted protein acidic and rich in cysteine and glypican-3 levels. *Clin Cancer Res.* 2005;11:8079–8088.
11. O'Neill DW, Adams S, Bhardwaj N. Manipulating dendritic cell biology for the active immunotherapy of cancer. *Blood.* 2004;104:2235–2246.
12. Steinman RM, Banchereau J. Taking dendritic cells into medicine. *Nature.* 2007;449:419–426.
13. Murphy A, Westwood JA, Teng MW, et al. Gene modification strategies to induce tumor immunity. *Immunity.* 2005;22:403–414.
14. Kaplan JM, Yu Q, Piraino ST, et al. Induction of antitumor immunity with dendritic cells transduced with adenovirus vector-encoding endogenous tumor-associated antigens. *J Immunol.* 1999;163:699–707.
15. Motomura Y, Senju S, Nakatsura T, et al. Embryonic stem cell-derived dendritic cells expressing glypican-3, a recently identified oncofetal antigen, induce protective immunity against highly metastatic mouse melanoma, B16-F10. *Cancer Res.* 2006;66:2414–2422.
16. Fairchild PJ, Brook FA, Gardner RL, et al. Directed differentiation of dendritic cells from mouse embryonic stem cells. *Curr Biol.* 2000;10:1515–1518.
17. Senju S, Hirata S, Matsuyoshi H, et al. Generation and genetic modification of dendritic cells derived from mouse embryonic stem cells. *Blood.* 2003;101:3501–3508.
18. Matsuyoshi H, Senju S, Hirata S, et al. Enhanced priming of antigen-specific CTLs in vivo by embryonic stem cell-derived dendritic cells expressing chemokine along with antigenic protein: application to antitumor vaccination. *J Immunol.* 2004;172:776–786.
19. Matsunaga Y, Fukuma D, Hirata S, et al. Activation of antigen-specific cytotoxic T lymphocytes by beta2-microglobulin or TAP1 gene disruption and the introduction of recipient-matched MHC class I gene in allogeneic embryonic stem cell-derived dendritic cells. *J Immunol.* 2008;181:6635–6643.
20. Fujii S, Shimizu K, Kronenberg M, et al. Prolonged IFN-gamma-producing NKT response induced with alpha-galactosylceramide-loaded DCs. *Nat Immunol.* 2002;3:867–874.
21. Senju S, Iyama K, Kudo H, et al. Immunocytochemical analyses and targeted gene disruption of GTPBP1. *Mol Cell Biol.* 2000;20:6195–6200.
22. Niwa H, Masui S, Chambers I, et al. Phenotypic complementation establishes requirements for specific POU domain and generic transactivation function of Oct-3/4 in embryonic stem cells. *Mol Cell Biol.* 2002;22:1526–1536.
23. Niwa H, Yamamura K, Miyazaki J. Efficient selection for high-expression transfectants with a novel eukaryotic vector. *Gene.* 1991;108:193–199.
24. Hirata S, Senju S, Matsuyoshi H, et al. Prevention of experimental autoimmune encephalomyelitis by transfer of embryonic stem cell-derived dendritic cells expressing myelin oligodendrocyte glycoprotein peptide along with TRAIL or programmed death-1 ligand. *J Immunol.* 2005;174:1888–1897.
25. Hirata S, Matsuyoshi H, Fukuma D, et al. Involvement of regulatory T cells in the experimental autoimmune encephalomyelitis-preventive effect of dendritic cells expressing myelin oligodendrocyte glycoprotein plus TRAIL. *J Immunol.* 2007;178:918–925.
26. Watarai H, Nakagawa R, Omori-Miyake M, et al. Methods for detection, isolation and culture of mouse and human invariant NKT cells. *Nat Protoc.* 2008;3:70–78.
27. Bohm W, Thoma S, Leithauser F, et al. T cell-mediated, IFN-gamma-facilitated rejection of murine B16 melanomas. *J Immunol.* 1998;161:897–908.
28. Matsuyoshi H, Hirata S, Yoshitake Y, et al. Therapeutic effect of alpha-galactosylceramide-loaded dendritic cells genetically engineered to express SLC/CCL21 along with tumor antigen against peritoneally disseminated tumor cells. *Cancer Sci.* 2005;96:889–896.
29. Overwijk WW, Tsung A, Irvine KR, et al. gp100/pmel 17 is a murine tumor rejection antigen: induction of "self"-reactive, tumoricidal T cells using high-affinity, altered peptide ligand. *J Exp Med.* 1998;188:277–286.
30. Hyoudou K, Nishikawa M, Umeyama Y, et al. Inhibition of metastatic tumor growth in mouse lung by repeated administration of polyethylene glycol-conjugated catalase: quantitative analysis with firefly luciferase-expressing melanoma cells. *Clin Cancer Res.* 2004;10:7685–7691.
31. Hyoudou K, Nishikawa M, Kobayashi Y, et al. Inhibition of adhesion and proliferation of peritoneally disseminated tumor cells by pegylated catalase. *Clin Exp Metastasis.* 2006;23:269–278.
32. Wilson MT, Johansson C, Olivares-Villagomez D, et al. The response of natural killer T cells to glycolipid antigens is characterized by surface receptor down-modulation and expansion. *Proc Natl Acad Sci USA.* 2003;100:10913–10918.
33. Harada M, Seino K, Wakao H, et al. Down-regulation of the invariant Valpha14 antigen receptor in NKT cells upon activation. *Int Immunol.* 2004;16:241–247.
34. Hyoudou K, Nishikawa M, Kobayashi Y, et al. PEGylated catalase prevents metastatic tumor growth aggravated by tumor removal. *Free Radic Biol Med.* 2006;41:1449–1458.
35. Massi D, Franchi A, Borgognoni L, et al. Osteonectin expression correlates with clinical outcome in thin cutaneous malignant melanomas. *Hum Pathol.* 1999;30:339–344.
36. Infante JR, Matsubayashi H, Sato N, et al. Peritumoral fibroblast SPARC expression and patient outcome with resectable pancreatic adenocarcinoma. *J Clin Oncol.* 2007;25:319–325.
37. Sangaletti S, Stoppacciaro A, Guiducci C, et al. Leukocyte, rather than tumor-produced SPARC, determines stroma and collagen type IV deposition in mammary carcinoma. *J Exp Med.* 2003;198:1475–1485.
38. Alvarez MJ, Prada F, Salvatierra E, et al. Secreted protein acidic and rich in cysteine produced by human melanoma cells modulates polymorphonuclear leukocyte recruitment and antitumor cytotoxic capacity. *Cancer Res.* 2005;65:5123–5132.
39. Banchereau J, Palucka AK, Dhodapkar M, et al. Immune and clinical responses in patients with metastatic melanoma to CD34(+) progenitor-derived dendritic cell vaccine. *Cancer Res.* 2001;61:6451–6458.
40. Wang B, He J, Liu C, et al. An effective cancer vaccine modality: lentiviral modification of dendritic cells expressing multiple cancer-specific antigens. *Vaccine.* 2006;24:3477–3489.
41. Kavanagh B, Ko A, Venook A, et al. Vaccination of metastatic colorectal cancer patients with matured dendritic cells loaded with multiple major histocompatibility complex class I peptides. *J Immunother.* 2007;30:762–772.
42. Mendiratta SK, Thai G, Eslahi NK, et al. Therapeutic tumor immunity induced by polyimmunization with melanoma antigens gp100 and TRP-2. *Cancer Res.* 2001;61:859–863.
43. Nieda M, Okai M, Tazbirkova A, et al. Therapeutic activation of Valpha24+Vbeta11+ NKT cells in human subjects results in highly coordinated secondary activation of acquired and innate immunity. *Blood.* 2004;103:383–389.
44. Ishikawa A, Motohashi S, Ishikawa E, et al. A phase I study of alpha-galactosylceramide (KRN7000)-pulsed dendritic cells in

patients with advanced and recurrent non-small cell lung cancer. *Clin Cancer Res.* 2005;11:1910–1917.
45. Chang DH, Osman K, Connolly J, et al. Sustained expansion of NKT cells and antigen-specific T cells after injection of alpha-galactosyl-ceramide loaded mature dendritic cells in cancer patients. *J Exp Med.* 2005;201:1503–1517.
46. Uchida T, Horiguchi S, Tanaka Y, et al. Phase I study of alpha-galactosylceramide-pulsed antigen presenting cells administration to the nasal submucosa in unresectable or recurrent head and neck cancer. *Cancer Immunol Immunother.* 2008;57:337–345.
47. Senju S, Suemori H, Zembutsu H, et al. Genetically manipulated human embryonic stem cell-derived dendritic cells with immune regulatory function. *Stem Cells.* 2007;25: 2720–2729.
48. Fukuma D, Matsuyoshi H, Hirata S, et al. Cancer prevention with semi-allogeneic ES cell-derived dendritic cells. *Biochem Biophys Res Commun.* 2005;335:5–13.
49. Takahashi K, Tanabe K, Ohnuki M, et al. Induction of pluripotent stem cells from adult human fibroblasts by defined factors. *Cell.* 2007;131:861–872.

Clinical & Experimental Immunology
The Journal of Translational Immunology

Clinical and Experimental Immunology ORIGINAL ARTICLE doi:10.1111/j.1365-2249.2009.03900.x

# Antigenic stimulation with cytochrome P450 2J expressed in mouse hepatocellular carcinoma cells regulates host anti-tumour immunity

S. Homma,* S. Koido,† Y. Sagawa,* H. Suzuki,† H. Komita,† E. Nagasaki,*† A. Takahara,*† J. Horiguchi-Yamada,* H. Tajiri,† D. C. Zeldin§ and T. Obata‡

*Departments of *Oncology and ‡Molecular Cell Biology, Institute of DNA Medicine, †Department of Internal Medicine, Jikei University School of Medicine, Tokyo, Japan, and §Division of Intramural Research, National Institute of Environmental Health Sciences, NC, USA*

Accepted for publication 9 January 2009
Correspondence: S. Homma, Department of Oncology, Institute of DNA Medicine, Jikei University School of Medicine, 3-25-8 Nishi-shimbashi, Minato-ku, Tokyo 105-8461 Japan.
E-mail: sahya@jikei.ac.jp

## Summary

Cytochrome P450 2J subfamily (CYP2J) enzymes expressed in mouse hepatocellular carcinoma (HCC) cells were identified as an antigen recognized by specific $CD4^+$ T cells and the structure of its T cell epitope was determined by proteomics-based exploration. The major histocompatibility complex (MHC) class II binding peptides were isolated from I-$A^k$/peptide complex of dendritic cells (DCs) loaded or unloaded with MIH-2 mouse HCC cells. MHC class II-binding peptides found in MIH-2-loaded DCs but not in unloaded DCs were determined by tandem mass spectrometric analysis. The peptide, consisting of amino acid 276–290 (DFIDAFLKEMTKYPE) of mouse CYP2J enzymes, was identified as an antigenic peptide presented in the context of MHC class II. Preventive treatment of mice with CYP2J peptide stimulated interferon (IFN)-γ production of splenocytes and suppressed the growth of implanted CYP2J-positive MIH-2 cells but not CYP2J-negative murine bladder tumour cells. However, continuous treatment of MIH-2-bearing mice with CYP2J peptide significantly suppressed IFN-γ production of splenocytes and accelerated the growth of implanted MIH-2 tumours *in vivo*. Increased frequencies of $CD4^+$forkhead box P3 regulatory T cells and $CD11b^+Gr\text{-}1^+$ myeloid suppressor cells were observed in splenocytes from the continuously immunized mice. These results indicate that antigenecity of CYP2J isoforms expressed in HCC cells activate host anti-tumour immunity at an initial stage of HCC, but suppress host anti-tumour immunity with excessive antigenic stimulation at an advanced stage.

**Keywords:** dendritic cell, immune regulation, liver cancer, MHC class II, $T_{reg}$

## Introduction

Host anti-tumour immunity could play an important role in the prevention of tumour development, and a tumour-associated antigen (TAA)-specific T cell response is one of the most important mechanisms for tumour rejection [1]. Crosti *et al.* have reported spontaneous reactivity to carcinoembryonic antigen (CEA) epitopes of peripheral blood $CD4^+$ T cells from patients with early CEA-positive lung cancer [2]. However, the immune system exhibits hyporesponsiveness or unresponsiveness to TAAs when tumours become large, resulting in further tumour development without immunological anti-tumour activity. Analysis of tumour-infiltrating lymphocytes has revealed antigen-specific hyporesponsiveness consistent with a form of T cell anergy [3]. Acquired tolerance to TAAs has been observed even when initial priming of T cells to TAAs was successful [4]. This immunosuppression might be caused by vascular endothelial growth factor (VEGF), interleukin (IL)-10, transforming growth factor (TGF)-beta or prostaglandin $E_2$ produced by tumour cells or tumour-associated immune cells, leading to generation of dysfunctional APCs inducing tolerance for T cell immunity [5,6]. Furthermore, tumour cells form a unique microenvironment to prevent immune attack [7].

Antigen-specific anti-tumour immunity might be inhibited by excessive antigenic stimulation with TAAs by a large tumour burden. In the case of $CD8^+$ T cells, low antigen levels lead to T cell deletion and high antigen levels lead to T cell tolerance [8]. Consequently, in advanced cancer, over-stimulation with immunogenic TAAs on tumour cells might paralyse anti-tumour immunity and favour tumour development. In order to prevent such immune paralysis induced by advanced cancer, it is necessary to identify TAAs


 

generating excessive antigenic stimulation on the host immune system.

$CD4^+$ T cell functions play a pivotal role in the induction of anti-tumour immunity, and T cell activation by stimulation with helper T cell epitopes is probably important for effective anti-cancer immune responses [9–11]. Meanwhile, it has been known that excessive antigenic stimulation with helper epitope peptide induces immune tolerance [12]. Although many TAAs recognized by specific $CD8^+$ cytotoxic T lymphocytes (CTLs) have been reported, fewer helper epitopes of TAAs have been identified than have CTL epitopes [2,13].

Recent progress in mass spectrometric analysis has enabled efficient TAA searches. Known, immunoprecipitated TAAs can be identified clearly with a proteometric approach [14]. Human leucocyte antigen class II presented peptides derived from tissue specimens of primary renal cell carcinoma have been analysed with mass spectrometry, and T helper epitopes from TAAs have been detected [15]. Dendritic cells (DCs), potent APCs, have been analysed with mass spectrometry to identify functional DC-associated molecules. Calreticulin was found with tandem mass spectrometric analysis to be a receptor of NY-ESO-1, a representative TAA, on DCs [16]. Röhn *et al.* have used nanoelectrospray ionization tandem mass spectrometry to examine DCs upon exposure to necrotic tumour cells and have identified melanotransferrin as a major histocompatibility complex (MHC) class II-restricted tumour antigen [17]. Mass spectrometric analysis could be applied to the detection of animal and human TAAs that would be presented by tumour-cell-captured APCs to T cells.

In this paper, we describe the identification of an immunostimulatory antigen expressed in mouse hepatocellular carcinoma (HCC) cells recognized by $CD4^+$ T cells which, in turn, suppress host anti-tumour immune activity through excessive antigenic stimulation. The antigen was identified with tandem mass analysis of MHC class II binding peptides isolated from DCs loaded with HCC cells.

## Materials and methods

### Mice, cell lines and reagents

Eight-week-old male C3H/HeNCrj mice were purchased from Charles River Japan (Yokohama, Japan). All animals received humane care in accordance with the US Public Health Service Policy on Humane Care and Use of Laboratory Animals.

A murine HCC cell line, MIH-2, was established in our laboratory from a liver tumour of a 15-month-old C3H/HeNCrj mouse [18]. Another mouse HCC cell line, Hepa 1–6, was purchased from the American Type Culture Collection (Manassas, VA, USA).

Monoclonal antibodies (mAbs) against murine CD11b and Gr-1 were purchased from BD Biosciences (San Jose, CA, USA). A kit for detecting $CD4^+$ forkhead box P3 transcription factor ($FoxP3^+$) regulatory T cells ($T_{regs}$) was purchased from eBioscience (San Diego, CA, USA). A mAb against $I\text{-}A^k$ for use in affinity chromatography was purchased from BD Biosciences. Rabbit polyclonal anti-CYP2J2pep3 antibody, which recognizes all known mouse cytochrome P450 2J subfamily (CYP2J) isoforms [19], and an anti-CYP2J6pep1 antibody, which is specific for mouse CYP2J6 [20], were kindly provided by Professor Darryl C. Zeldin (National Institute of Environmental Health Sciences, National Institutes of Health, Bethesda, MD, USA).

### Preparation of DCs loaded with MIH-2 cells

The preparation of DCs loaded with MIH-2 cells was performed as described previously [18,21]. Briefly, DCs were prepared from bone marrow cells of 8–10-week-old male C3H/HeNCrj mice. Then $2 \times 10^7$ DCs were mixed with $10^7$ irradiated MIH-2 cells and centrifuged. After the supernatant had been discarded, 0·5 ml of 50% polyethylene glycol (PEG) (PEG 1450; Sigma-Aldrich, St Louis, MO, USA) was added to the cell pellet, which was left for 1 min at room temperature, after which the PEG solution was diluted gradually. After removal of PEG by centrifugation and overnight incubation, non-adherent or loosely attached cells were collected with gentle pipetting as DCs loaded with MIH-2 cells (DC/MIH-2) and used for isolation of peptides fixed with $I\text{-}A^k$ molecules.

### Affinity column chromatography

Cell pellets of PEG-treated cells were suspended in TNE buffer (10 mM Tris, 1% Nonidet P-40, 0·15 M NaCl, 1 mM ethylenediamine tetraacetic acid, pH 8·0) and sonicated for 30 s. The supernatant, obtained by centrifugation at 10 000 ***g*** for 15 min, was applied to a column containing anti-$I\text{-}A^k$ antibody-coated Formyl-Cellulofine beads (Seikagaku Corporation, Tokyo, Japan) equilibrated with phosphate-buffered saline (PBS), after which the column was washed with PBS until A280 absorbance disappeared. The column was prewashed with 0·5 M NaCl and then washed with elution buffer (0·2 M glycine-HCl, pH 2·5). Each 0·5 ml of the eluted samples was collected and examined for A280 absorbance.

### Preparation of peptide samples and tandem mass spectrometric analysis

The peptide sample fraction was applied to solid-phase extraction for concentrating peptides and removing detergents. An Octadecyl-Silica SepPack column (Waters Corp., Milford, MA, USA) was activated with 4 ml of methanol and equilibrated with 2 ml of water. After the sample fraction was applied, the SepPack column was washed with water (4 ml) and eluted with an 80% (V/V) acetonitrile

aqueous solution containing 0·1% (V/V) formic acid. The organic solvent fraction was frozen and lyophilized. The resulting cloudy precipitate was resolved with 80% (V/V) methanol containing 0·1% (V/V) formic acid. After centrifugation at 16 000 ***g*** for 10 min, the 2-μl aliquot was placed in a microcapillary of the nanospray apparatus of the tandem mass spectrometry system.

A Q-Trap tandem mass spectrometer (Applied Biosystems, Foster City, CA, USA) equipped with nanospray systems was used. The BioAnalyst (version 1·3) data-analysis software system (Applied Biosystems) was used for assaying optimization and analysis with tandem mass spectrographs.

Peak reconstruction of mass spectra was recorded under m/z 1500, and the chosen peptide peaks were analysed with tandem mass spectrometric analysis after passage through a nitrogen gas collision chamber. To determine amino acid sequences in tandem mass spectra, the peaks were analysed with automated sequence Tag determination and a database search performed with the data-analysis software.

### Reverse transcriptase–polymerase chain reaction

Total RNA was extracted using Isogen (Nippongene, Toyama, Japan), according to the manufacturer's instructions. RNA was reverse-transcribed with Moloney murine leukaemia virus RT (Invitrogen Corp., Carlsbad, CA, USA) and complementary DNA was subjected to the polymerase chain reaction (PCR) with *Taq* polymerase (Takara Biochemical, Tokyo, Japan) in a thermal cycler. Primers were designed as follows: mouse CYP2J6, forward GTATTTG GAGACAACAATGATTAGTCAGC, reverse TATCAGCAAG TCTTGCTGCCCTCTTC [expected size of the product was 407 base pairs (bp)]; mouse CYP2J9, forward TGTTTGG AGTCATCAATGATGTGC, reverse CGGTCTGCCAGATTC GGCTGTCTTGC (410 bp); and mouse CYP2J11, forward TGTTCTGAGGCATCAATGATGTCAGT, reverse TGGTCA TCTAAGGTTGGGTGTCTCCCA (410 bp).

### Immunoblot analysis

Proteins were separated by sodium dodecyl sulphate-polyacrylamide gel electrophoresis, and transferred to polyvinylidene fluoride membranes (Bio-Rad Laboratories, Hercules, CA, USA). After blocking in Tris-buffered saline with Tween-20 [25 mM Tris-HCl (pH 8·0), 150 mM Nacl, 0·1% Tween 20] with 10% Difco skimmed milk (BD Biosciences Diagnostic Systems, Sparks, MA, USA), the membranes were incubated with anti-CYP2J2pep3 or anti-CYP2J6pep1 antibodies. Each membrane was then probed for 90 min with peroxidase-conjugated anti-rabbit Ig (Bio-Rad Laboratories) and analysed with an enhanced chemiluminescence detection system (Amersham Biosciences, Little Chalfont, Buckinghamshire, UK).

### Vaccination of mice with CYP2J peptide

The CYP2J peptide (NH2-DFIDAFLKEMTKYPE-COOH) and control ovalbumin (OVA) peptide (NH2-GGLEPINFQTAADQA-COOH) were synthesized by Funakoshi Co. Ltd (Tokyo, Japan). The purity of the each peptide was 95·81% and 96·05% respectively. OVA was used as a negative control for MHC class II presented immunogenic antigen. CYP2J peptide or OVA peptide (20 μg/20 μl $H_2O$) was mixed with 0·2 ml of $H_2O$ and 0·2 ml of complete Freund's adjuvant (Difco Laboratories, Detroit, MI, USA), agitated vigorously to generate emulsion, and injected subcutaneously once a week.

For preventive treatment of mice with CYP2J peptide, naive mice were immunized twice with the peptide and tumour cells were implanted 1 week after immunization. For continuous treatment of MIH-2-bearing mice with the peptide, immunization started 1 week after the implantation of tumour cells.

### Production of cytokines by splenocytes

Splenocytes from untreated control or peptide-vaccinated mice were collected and cultured in 24-well culture plates ($5 \times 10^6$/well) for 72 h. In some experiments, CYP or OVA peptide (20 μg/ml) was added to the culture to stimulate T cells *in vitro*. Supernatants were collected and examined for interferon (IFN)-γ, IL-4, IL-10 and TGF-beta using an enzyme-linked immunosorbent assay kit (Biosource International).

## Results

### Identification of MIH-2-derived MHC class II binding peptide from DCs loaded with MIH-2 cells by mass spectrometric analysis

Tandem mass spectrometry was performed to find peptide peaks of 12–15 amino acids, suitable for binding to MHC class II molecules, from MIH-2-loaded DCs. However, we found no objective ion peaks of 12–15 amino acid peptides. It is probable that isolated MHC class II binding peptides were digested by endogenous peptidases. We then searched for smaller peptide peaks and some ion peaks of peptides were found with total ion chromatography of MIH-2-loaded DCs which were not found in control DCs (Fig. 1). A representative ion peak, indicated by an arrow in Fig. 1 (m/z 821·8), was analysed further using the tandem mass system, and its structural amino acid sequence was determined to be EMTK.

Database analysis revealed that the EMTK polypeptide corresponded to amino acids 284–287 of several enzymes of mouse cytochrome P450 2J (CYP2J) (Fig. 2). Two other candidate molecules, mouse nucleolin (amino acids 285–288)

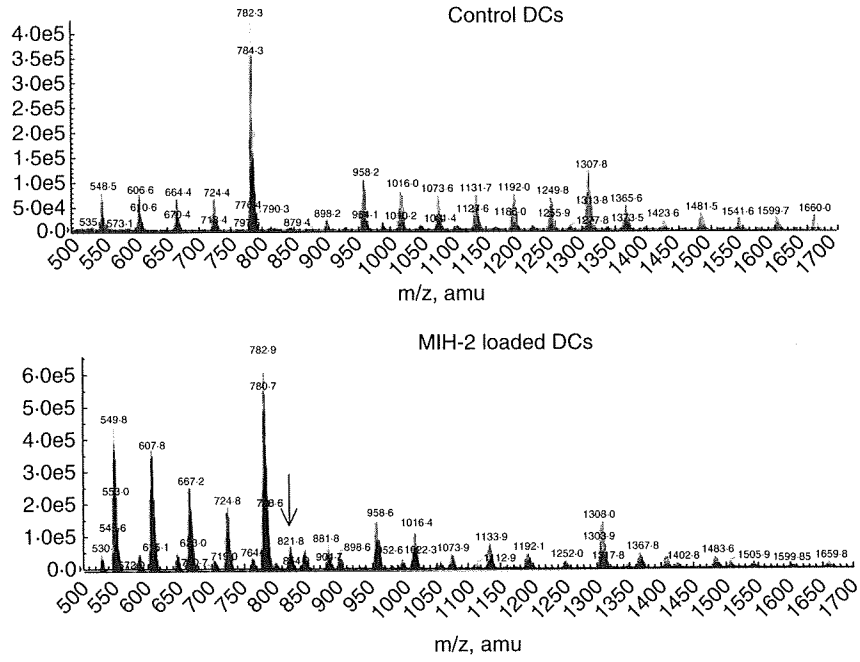


**Fig. 1.** Total ion chromatograph of I-A$^k$ binding peptides derived from control dendritic cells (DCs) (upper) or MIH-2-loaded DCs (lower). Control DCs, treated with 50% polyethylene glycol (PEG) alone, or MIH-2 loaded-DCs, generated by treatment of mixture of DCs and MIH-2 cells with 50% PEG, as described in Materials and methods, were treated with detergent, and I-A$^k$/peptide complexes were obtained with anti-I-A$^k$ affinity column chromatography.
Each binding peptide was analysed with liquid chromatography/mass spectrometry. A representative peptide ion peak that was found only in peptides from MIH-2-loaded DCs and not those from control DCs, indicated by an arrow (821·8 m/z), was analysed further with liquid chromatography/tandem mass spectrometry.

and queuine tRNA-ribosyltransferase (amino acids 200–203), which contain EMTK in their amino acid sequences, were also identified. The I-A$^k$ binding motif structure (DFIDAFLK) was found in amino acids 276–283 of CYP2Js, adjacent to EMTK (Fig. 2), suggesting that a peptide consisting of 15 amino acids, including the I-A$^k$ binding motif and EMTK (DFIDAFLKEMTKYPE) of CYP2Js, would be presented by MIH-2–loaded DCs to CD4$^+$T cells. Mouse nucleolin did not possess a I-A$^k$ binding motif adjacent to EMTK, and mouse queuine tRNA-ribosyltransferase had lower possibility score, indicating that CYP2J is the most possible candidate molecule.

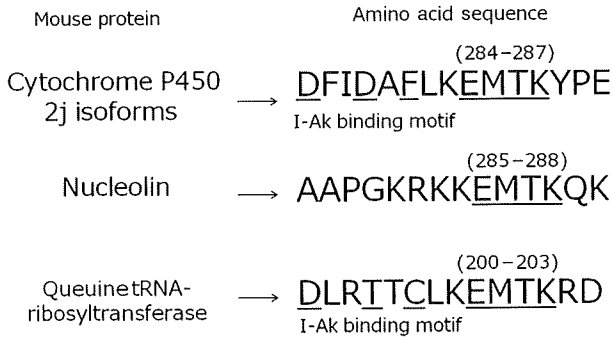


**Fig. 2.** Amino acid sequence of mouse CYP2J6 and a possible epitope recognized by specific CD4$^+$ T cells in the context of major histocompatibility complex (MHC) class II. EMTK (284E–287K) was detected from the peptides binding to I-A$^k$ of MIH-2-loaded dendritic cells (DCs) with tandem mass analysis (TMA). D276–K283, adjacent to EMTK on the N-terminal side, possesses the I-A$^k$ binding motif. A peptide consisting of 15 amino acids containing the I-A$^k$ binding motif and EMTK, as indicated by an underline, was synthesized and examined for further biological activity.

## Expression of CYP2Js in HCC cells and normal liver cells

Messenger RNA (mRNA) encoding CYP2J6 was found with reverse transcriptase (RT)–PCR to be expressed in MIH-2 HCC cells as well as Hepa 1–6 HCC cells, B16 melanoma cells and LY-R lymphoma cells (Fig. 3). It was also expressed in C26 cells at a very low level. The enzymes CYP2J6, CYP2J9 and CYP2J11 each contain EMTK, but CYP2J2, CYP2J4, CYP2J5 and CYP2J13 do not [19,20,22]. The mRNA encoding CYP2J9 was expressed in MIH-2 cells at a very low level, and the mRNA encoding CYP2J11 was not expressed in

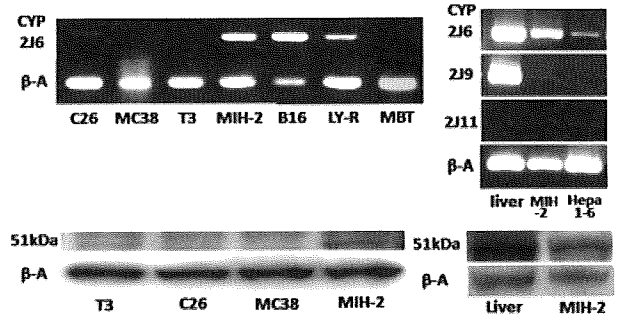


**Fig. 3.** Expression of CYP2J mRNA and protein in various tumour cell lines and normal liver tissue. Expression of mRNA encoding CYP2J6, 2J9 and 2J11 was examined with reverse transcription–polymerase chain reaction, as described in Materials and methods (upper). Expression of CYP2J protein (51 kDa) recognized by anti-CYP2J2pep3 antibody was examined with immunoblot analysis (lower). C26 and MC38, mouse colon cancer; T3, mouse small intestine tumour; MIH-2 and Hepa 1–6, mouse hepatocellular carcinoma; B16, mouse melanoma; LY-R, mouse lymphoma; β-A, beta-actin.

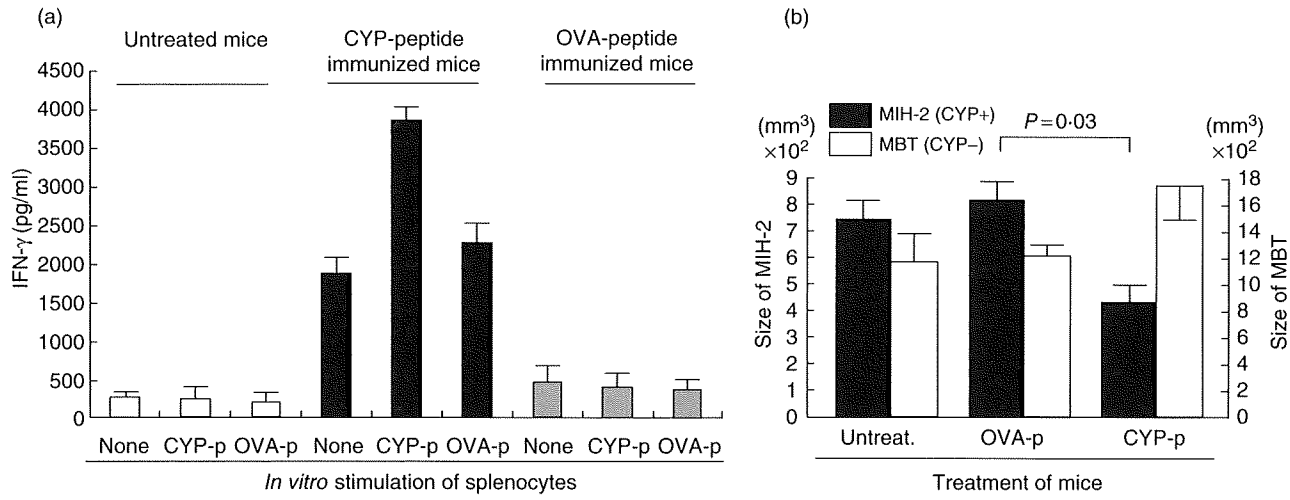


**Fig. 4.** (a) CYP2J peptide was immunogenic in naive C3H/HeN mice. Male C3H/HeN mice received subcutaneous injections of CYP2J peptide (20 μg/mouse) with adjuvant on days 1 and 7. Splenocytes were collected on day 14 and cultured for 72 h with or without CYP peptide (20 μg/ml) or control ovalbumin (OVA) peptide (20 μg/ml). Supernatants were examined for interferon (IFN)-γ with enzyme-linked immunosorbent assay. (b) Immunization with CYP2J peptide suppressed the growth of implanted MIH-2 cells *in vivo*. Male C3H/HeN mice received subcutaneous injections of CYP2J peptide (20 μg/mouse) or OVA peptide (20 μg/mouse) with adjuvant on days 1 and 7. On day 14, the immunized mice were implanted subcutaneously with MIH-2 cells ($10^6$/mouse) or murine bladder tumour (MBT) cells ($10^6$/mouse), and the tumour size (long diameter × short diameter) was measured 4 weeks after the tumour cell implantation. CYP2J was detectable in MIH-2 cells but not in MBT cells by immunoblot analysis.

either normal liver or MIH-2 cells (Fig. 3). CYP2J protein (51 kDa) was recognized with an anti-CYP2J2pep3 antibody in MIH-2 cells but not in T3, C26 or MC38 cells on Western blotting analysis (Fig. 3).

### Preventive treatment of naive mice with CYP2J peptide stimulated IFN-γ production of splenocytes and suppressed the growth of implanted MIH-2 cells *in vivo*

Splenocytes from mice immunized twice with CYP2J peptide (DFIDAFLKEMTKYPE) showed significantly higher IFN-γ production *in vitro* than did splenocytes from untreated mice or mice immunized with OVA peptide (Fig. 4a). Furthermore, production of IFN-γ by splenocytes from CYP2J peptide-immunized mice was enhanced when CYP2J peptide, but not OVA peptide, was added to the culture (Fig. 4a). In contrast, production of IL-4 by splenocytes was not enhanced (data not shown).

When MIH-2 cells ($CYP2J^+$) were implanted into mice immunized with CYP2J peptide, tumour growth was suppressed significantly (Fig. 4b). However, growth of implanted murine bladder tumour cell ($CYP2J^-$, as shown in Fig. 3) was not suppressed by immunization with CYP2J peptide (Fig. 4b).

### Repeated immunization of MIH-2-bearing mice with CYP2J peptide suppressed IFN-γ production and accelerated MIH-2 tumour growth *in vivo*

The immunostimulatory capacity of CYP2J peptide was studied through repeated immunization of naive mice. Production of IFN-γ by splenocytes increased in mice immunized one to six times (Fig. 5). In contrast, IFN-γ production was suppressed when mice were immunized seven and eight times (Fig. 5). These results suggest that excessive immunization (more than six times) with CYP2J peptide can induce unresponsiveness or anergy to CYP2Js.

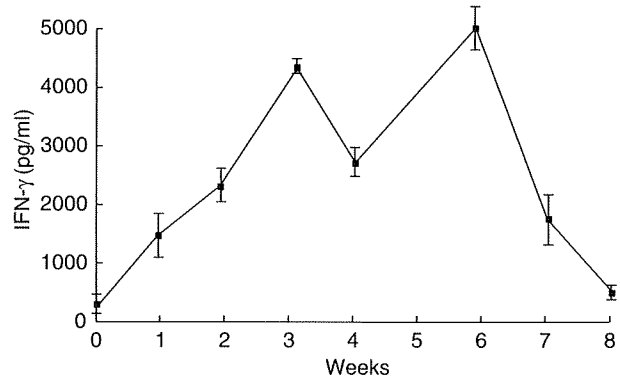


**Fig. 5.** Enhancement of interferon (IFN)-γ production of splenocytes by moderate immunization with CYP2J peptide but suppression by excessive immunization. CYP2J peptide (20 μg/mouse) with adjuvant was injected subcutaneously once a week. Splenocytes were obtained from mice 3 days after each vaccination. Splenocytes ($5 \times 10^6$/ml) were incubated for 72 h and supernatants were examined for IFN-γ by enzyme-linked immunosorbent assay ($n = 3$). Splenocytes from control mice injected with phosphate-buffered saline were collected at each time-point and their IFN-γ production was 200–350 pg/ml ($n = 3$).

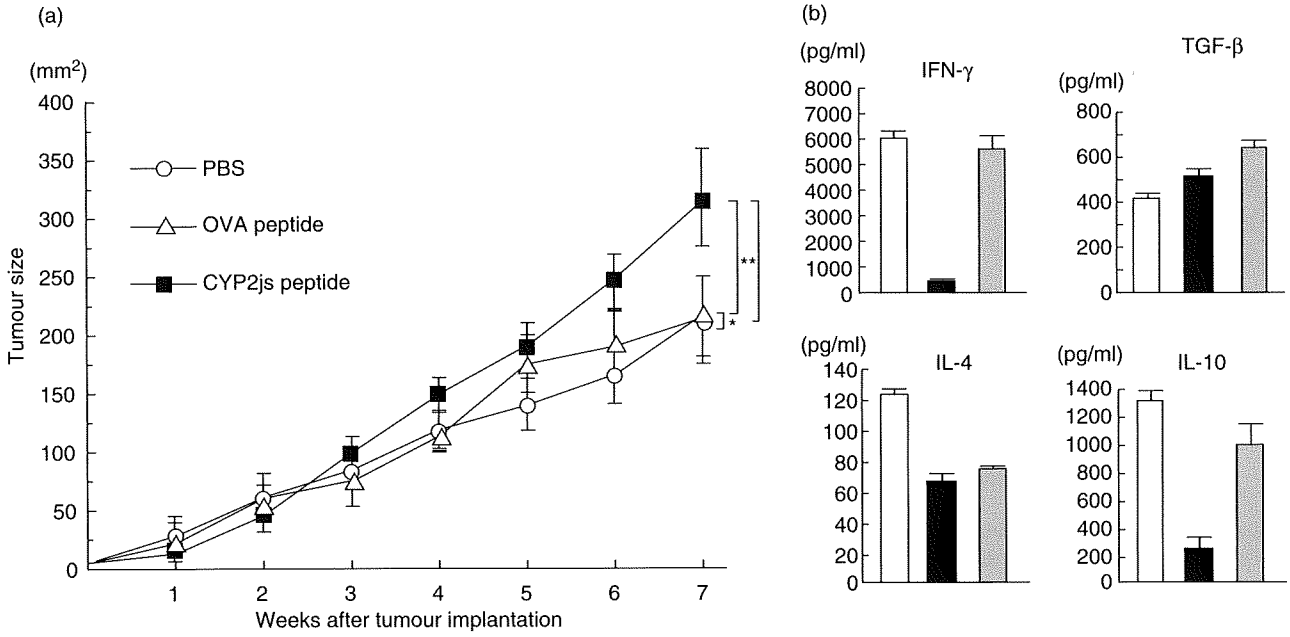


**Fig. 6.** (a) Repeated immunization of MIH-2-bearing mice with CYP2J peptide accelerated MIH-2 tumour growth *in vivo*. MIH-2 cells ($2 \times 10^6$/mouse) were implanted into female C3H/HeN mice, which were immunized with CYP2J peptide or control ovalbumin (OVA) peptide (20 μg/mouse) with adjuvant once a week after MIH-2 cell implantation. Tumour size (long diameter × short diameter) was measured every week. Open circle, mice treated with phosphate-buffered saline (PBS); open triangle, mice immunized with OVA peptide; closed square, mice immunized with CYP2J peptide. $^*P = 0{\cdot}8692$, $^{**}P = 0{\cdot}0261$, $^{***}P = 0{\cdot}0075$ determined with repeated-measures analysis of variance ($n = 6$). This is a representative result of three replicated experiments. (b) Cytokine production of splenocytes from MIH-2-bearing mice immunized excessively (seven times) with CYP2J peptide. Splenocytes were collected and cultured at $5 \times 10^6$ cells/ml for 72 h. Supernatants were examined for interferon-γ, interleukin (IL-4), IL-10 and transforming growth factor-β. Open columns, MIH-2-bearing mice treated with PBS; closed columns, MIH-2 bearing mice immunized with CYP2J peptide; shaded columns, MIH-2-bearing mice immunized with OVA peptide.

Mice bearing MIH-2 tumours and immunized excessively with CYP2J peptide exhibited a significant enhancement of tumour growth compared with mice treated with PBS (Fig. 6a). However, immunization with control OVA peptide did not enhance tumour growth. These results indicate that excessive immunization of MIH-2-bearing mice with CYP2J peptide suppresses host anti-tumour immunity against MIH-2 cells.

Splenocytes from MIH-2-bearing mice, even 7 weeks after MIH-2 cell implantation, showed considerable IFN-γ production *in vitro* by immune stimulation with implanted MIH-2 cells (Fig. 6b). Production of IFN-γ by splenocytes from MIH-2-bearing mice was also suppressed markedly by excessive immunization with CYP2J peptide (Fig. 6b).

Production of IL-4, IL-10 and TGF-beta by splenocytes from mice immunized excessively with CYP2J was examined. Production of IL-10 was suppressed by excessive immunization with CYP2J peptide and IL-4 production was suppressed by CYP2J and OVA peptide, but TGF-beta production was not affected (Fig. 6b). Therefore, suppression of IFN-γ production was not induced by the shift from the T helper type 1 (Th1) to the Th2 immune environment or by enhanced production of immunosuppressive IL-10 or TGF-beta.

## Increased frequency of immunosuppressive cells in splenocytes from mice immunized excessively with CYP2J peptide

Splenocytes from mice immunized excessively with CYP2J peptide were examined for the frequency of immunosuppressive cells: $CD4^+$ $FoxP3^+$ $T_{regs}$. Splenocytes from MIH-2-bearing mice showed an almost twofold increase in the frequency of $CD4^+FoxP3^+$ $T_{regs}$ (Fig. 7a). Mice that had been immunized excessively with CYP2J peptide showed increased frequency of $T_{regs}$ in splenocytes even without MIH-2 cell implantation. However, excessive immunization of MIH-2-bearing mice with CYP2J peptide did not increase the $T_{reg}$ frequency further.

The frequency of $CD11b^+Gr\text{-}1^+$ myeloid suppressor cells (MSCs) was also increased significantly in mice immunized excessively with CYP2J peptide (Fig. 7b). The frequencies of MSCs in each treated group were 8·58 ± 2·11 (non-MIH-2-bearing mice treated with PBS), 23·46 ± 5·56 (non-MIH-2-bearing mice immunized with CYP2J peptide), 7·89 ± 2·89 (MIH-2-bearing mice treated with PBS) and 18·34 ± 4·10 (MIH-2-bearing mice immunized with CYP2J peptide) ($n = 3$). No increase in the frequencies of $T_{regs}$ and MSCs was observed in mice bearing or non-bearing

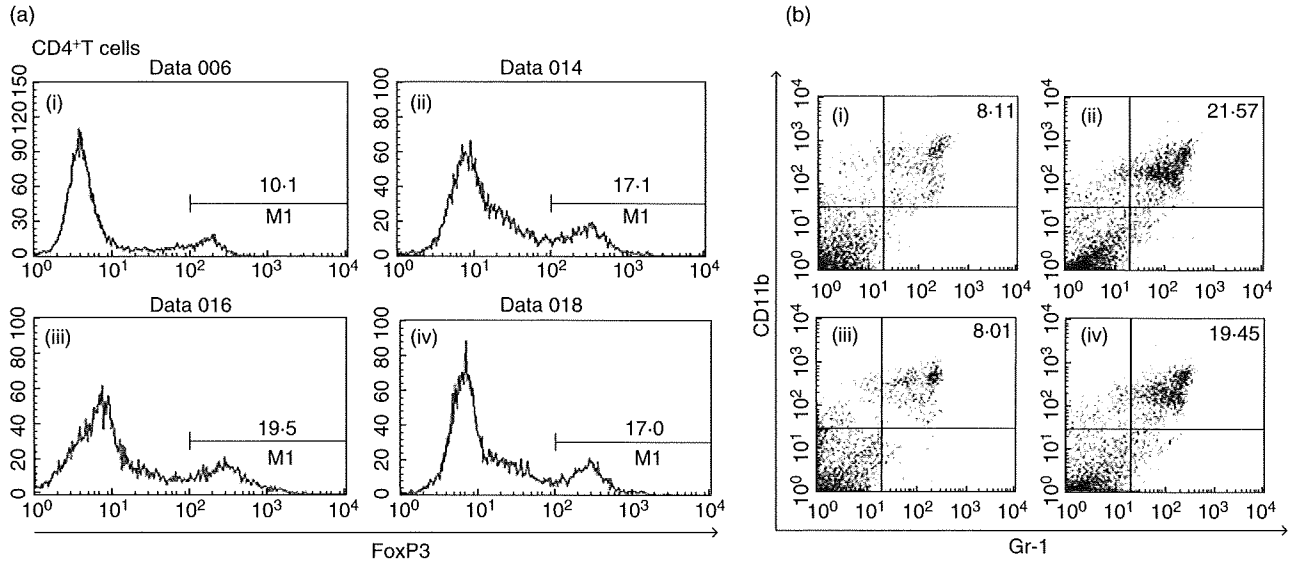


**Fig. 7.** (a) Frequency of forkhead box P3 (FoxP3$^+$) cells in splenic CD4$^+$ T cells from MIH-2-bearing mice or non-tumour-bearing mice immunized excessively with CYP2J peptide. Splenocytes were collected from each group of mice, and CD4$^+$ T cells were obtained by magnetic sorting. The frequency of FoxP3$^+$ cells in CD4$^+$ T cells was examined with flow cytometry. (i) Non-MIH-2-bearing mice treated with phosphate-buffered saline (PBS); (ii) non-MIH-2-bearing mice immunized with CYP2J peptide 7 times; (iii) MIH-2-bearing mice treated with PBS; (iv) MIH-2-bearing mice immunized seven times with CYP2J peptide. (b) Frequency of CD11b$^+$Gr-1$^+$ cells in splenocytes from MIH-2-bearing mice or non-MIH-2-bearing mice immunized excessively with CYP2J peptide. Splenocytes were collected from each group of mice, stained with fluorescein isothiocyanate-conjugated monoclonal antibodies (mAbs) to Gr-1 and with phycoerythrin-conjugated mAbs to CD11b, and analysed with two-colour flow cytometry. (i) Non-MIH-2-bearing mice treated with PBS; (ii) non-MIH-2-bearing mice immunized seven times with CYP2J peptide; (iii) MIH-2-bearing mice treated with PBS; (iv) MIH-2-bearing mice immunized seven times with CYP2J peptide.

MIH-2 tumour immunized with OVA peptide (data not shown).

## Discussion

Splenocytes from mice immunized twice with CYP2J peptide showed significantly high IFN-γ production *in vitro*, and it was enhanced further when CYP2J peptide was added to the culture. These results indicate that CYP2J peptide is immunogenic for naive immunocompetent mice and that adequate immunization with CYP2J peptide can activate the Th1 immune condition. CYP2Js antigenicity providing Th1 might contribute to MIH-2 tumour rejection because MIH-2 cells are susceptible to IFN-γ and to the cytotoxic activity of macrophages activated by IFN-γ[18,23].

The CYP2Js are newly discovered CYP subfamily enzymes that are involved in arachidonic acid metabolism; however, little is known about the role of CYP2Js in immunology. Ma *et al.* [20] have reported that because the turnover of CYP2J6 in tissue is extremely rapid, the mRNA of only CYP2J6 can be detected with RT–PCR but that CYP2J6 protein cannot be detected with immunoblot analysis. In the present study, we could not detect CYP2J6 protein in MIH-2 cells or normal liver tissue with immunoblot analysis using a CYP2J6-specific anti-CYP2J6pep1 antibody, although these tissues expressed mRNA encoding CYP2J6. It is possible that CYP2Js in normal tissue might have an unusual turnover *in vivo* which prevents the formation of naturally processed epitopes for immune recognition. Normal hepatocytes under non-pathological conditions would not release CYP2J to the outside of the cells. However, if CYP2J-expressing tumour cells did release CYP2J, it might be recognized as just a 'non-self' antigen by the immune system, because the immune system had never encountered the antigenic CYP2J epitope because of its rapid destruction. There is a concern that immunization with CYP2J peptide might induce autoimmune hepatic inflammation by activation of autoreactive T cells responsive to hepatocytes. It was found that about 10% of the vaccinated mice showed mild hepatic inflammation by histological examination of the liver without elevation of liver-derived enzymes such as alanine aminotransferase in sera. This mild liver inflammation might be caused by the action of IFN-γ produced by the activated CD4$^+$ T cells, and antigen-specific activation of CD8$^+$ CTLs would be required for the generation of significant autoimmune liver inflammation.

Considering that splenocytes from MIH-2-bearing mice showed high IFN-γ production, CYP2Js released from MIH-2 tissue might stimulate host anti-tumour immunity to produce IFN-γ. MIH-2 tumours might not develop if tumour cells undergo apoptosis through the direct action of IFN-γ or the cytotoxic activity of IFN-γ-activated immune cells. However, once tumour cells evade IFN-γ-mediated

immune attack and continue to proliferate, the large tumour burden would provide excess antigenic stimulation to the host immune system, deleting CYP2J-specific T cells by activation-induced cell death [24], accelerating tumour growth. Using a preclinical mouse model, Sotomayor *et al.* [25] have shown anergy of $CD4^+$ TAA-specific T cells that correlates with a lack of tumour rejection *in vivo*. Because anti-tumor activity against MIH-2 tumours is mediated by direct cytotoxicity of IFN-γ or IFN-γ-activated macrophages [18,23], suppression of IFN-γ production of $CD4^+$ T cells must favour the development of MIH-2 tumours.

The $T_{regs}$ with immunosuppressive activity can be characterized by cell-surface co-expression of CD4 and CD25 [26] and by co-expression of FoxP3 [27]. $T_{regs}$ are defined functionally as T cells that inhibit immune response by diminishing the activity of other cell types through direct or indirect modes of action [27–29]. Our present results suggest strongly that an increase in $T_{regs}$ is associated closely with excessive antigenic stimulation with CYP2J. $T_{regs}$ mediate peripheral tolerance by suppressing self-antigen-reactive T cells [5,30]. Because most TAAs are self-antigens, suppression of TAA-specific lymphocytes by $T_{regs}$ has been proposed as a mechanism for the failure of anti-tumour immunity [31,32]. Immunization with autoantigens identified through serological identification of antigens by recombinant expression cloning (SEREX) has been reported to activate $CD4^+CD25^+$ $T_{regs}$ [33]. Furthermore, immunization with SEREX-defined autoantigens suppressed anti-tumour immunity and accelerated chemically induced tumour development [34]. Accordingly, it seems likely that excessive antigenic stimulation with some $CD4^+$ T cell epitopes of autoantigens, including TAAs, might induce immune tolerance or unresponsiveness preferentially.

Several studies have shown that the number of MSCs is increased markedly in the peripheral blood of tumour-bearing animals and of patients with cancer, whereas the number of DCs is decreased [35]. Up-regulation of signal transducer and activator of transcription-3 and secretion of tumour-derived cytokines, such as VEGF, TGF-beta, granulocyte–macrophage colony-stimulating factor, IL-10 and prostaglandin, have been shown to arrest differentiation of APCs from their myeloid progenitors and trigger accumulation of MSCs [36,37]. MSCs induce immunosuppression through two enzymes involved in arginine metabolism: inducible nitric oxide (NO) synthetase 2, which generates NO, and arginase 1, which depletes L-arginine, generating amino acid starvation for T cell activation [38]. Tumour-associated MSCs have been reported recently to mediate the development of tumour-induced $T_{regs}$ and T cell anergy in tumour-bearing hosts [39]. $T_{regs}$ are differentiated by stimulation with dysfunctional DCs or APCs that are generated in a tumour microenvironment with abundant VEGF, IL-10 or TGF-beta [5,6]. Tumours convert DCs into TGF-beta-expressing immature myeloid DCs that can promote $T_{reg}$ proliferation [40].

Collectively, CYP2J isoforms expressed in HCC cells activate anti-tumour immunity with low or moderate antigenic stimulation but suppress anti-tumour immunity with excessive antigenic stimulation. Immune suppression provided by over-stimulation with CYP2J antigenicity was associated closely with induction of $CD4^+FoxP3^+$ $T_{regs}$ and $CD11b^+Gr\text{-}1^+$ MSCs. Excessive immune stimulation with CYP2J derived from HCC cells would suppress host anti-tumour immunity, leading to further tumour development in advanced stages of HCC.

## Acknowledgements

This work was supported by Grants-in-Aid for Scientific Research (C) and (B), and a Grant-in-Aid for Exploratory Research from the Ministry of Education, Culture, Sports, Science and Technology of Japan, Grants-in-Aid from the Japan Medical Association, the Takeda Science Foundation, the Pancreas Research Foundation of Japan, the Jikei University Research Fund, the Promotion and Mutual Aid Corporation for Private School of Japan and the Science Research Promotion Fund. This work was also supported, in part, with funds from the Intramural Research Program of the NIH, National Institute of Environmental Health Sciences.

## References

1 Finn OJ. Cancer immunology. N Engl J Med 2008; **358**:2704–15.
2 Crosti M, Longhi R, Consogno G, Melloni G, Zannini P, Protti MP. Identification of novel subdominant epitopes on the carcinoembryonic antigen recognized by CD4+ T cells of lung cancer patients. J Immunol 2006; **176**:5093–9.
3 Guilloux Y, Viret C, Gervois N *et al.* Defective lymphokine production by most CD8+ and CD4+ tumor-specific T cell clones derived from human melanoma-infiltrating lymphocytes in response to autologous tumor cells *in vitro*. Eur J Immunol 1994; **24**:1966–73.
4 Anderson MJ, Shafer-Weaver K, Greenberg NM, Hurwitz AA. Tolerization of tumor-specific T cells despite efficient initial priming in a primary murine model of prostate cancer. J Immunol 2007; **178**:1268–76.
5 Zou W. Immunosuppressive networks in the tumour environment and their therapeutic relevance. Nat Rev Cancer 2005; **5**:263–74.
6 Gabrilovich D. Mechanisms and functional significance of tumour-induced dendritic-cell defects. Nat Rev Immunol 2004; **4**:941–52.
7 Gajewski TF. Identifying and overcoming immune resistance mechanisms in the melanoma tumor microenvironment. Clin Cancer Res 2006; **12**:2326s–30s.
8 Redmond WL, Marincek BC, Sherman LA. Distinct requirements for deletion versus anergy during CD8 T cell peripheral tolerance *in vivo*. J Immunol 2005; **174**:2046–53.
9 Topalian SL. MHC class II restricted tumor antigens and the role of CD4+ T cells in cancer immunotherapy. Curr Opin Immunol 1994; **6**:741–5.
10 Wang RF. The role of MHC class II-restricted tumor antigens and CD4+ T cells in antitumor immunity. Trends Immunol 2001; **22**:269–76.